Hydrogen ion irradiation of various minerals simulating the space weathering.

Haruka Uchida[1], *Aki Takigawa[1,2], Akira Tsuchiyama[1], Kohtaku Suzuki[3], Yoshinori Nakata[3], Akira Miyake[1], Akiko Takayama[1]

1. Division of Earth and Planetary Science, Kyoto University, 2. The Hakubi Center for Advanced Research, Kyoto University, 3. The Wakasa Wan Energy Research Center

The space-weathering on air-less bodies is caused by solar-wind irradiation and bombardment of micrometeorites [1, 2]. The space-weathered rims such as amorphous layers and blisters on the surface were observed on regolith particles from Lunar and asteroid Itokawa [3, 4]. There are limited irradiation experiments of minerals by hydrogen ions, which is the dominant gas species in the solar wind [e.g., 5]. In this study, we performed irradiation experiments of hydrogen ions to carious minerals to examine the difference of surface structure changes due to ion irradiation between materials with different crystal structures and chemical compositions.

The target materials for ion irradiation are forsterite (Fo_{100}, syn.), olivine (Fo_{92}, San Carlos, USA) , enstatite (En_{99}, Tanzania), spinel($MgAl_2O_4$, syn.), corundum (Al_2O_3, syn.), enstatite glass($MgSi_{0.97}Al_{0.03}O_3$, syn.), serpentine (Mg#=0.98, South India) , pyrrhotite ($Fe_{0.90}S$, Chihuahua, Mexico), iron meteorite ((Fe, Ni), Nantan meteorite (IIICD)). Samples are mechanically polished and cut into 3×5×0.5 mm rectangles. The damaged layers due to polishing were removed by chemical polishing with colloidal silica.

Experiments were carried out with the low-energy ion implantation equipment in The Wakasa Wan Energy Research Center. The samples were irradiated by 40 keV H_2^+ ions (corresponding to 20 keV H^+ ions) with the doses of 10^{16}, 10^{17}, and 10^{18} ions/cm^2. The cooling stages were used for experiments longer than 60 min to keep the samples at room temperature. We observed the surfaces of the irradiated samples with with an FE-SEM (JEOL JSM 7001F). FIB-lift-out sections were prepared with an FE-FIB (FEI Helios NanoLab 3G CX) and observed with FE-TEM (JEOL JEM 2100F).

We observed forsterite, olivine, and pyrrhotite irradiated by hydrogen ions with a dose of 10^{18} ions/cm^2, and irradiated enstatite with dosed of 10^{17} and 10^{18} ions/cm. The TEM observation showed that vesicles were observed under blisters on irradiated enstatite with a dose of 10^{18} ions/cm. The crystal structure of orthoenstatite remained in the very surface of the blister skin. An amorphous structure was observed just above the vesicles. The irradiated enstatite with a dose of 10^{17} ions/cm only showed a slight deformation of the crystal structure. These observation shows that the threshold dose of the enstatite amorphization by 20 keV hydrogen ion irradiation is between 10^{17} and 10^{-18} ions/cm^2. We did not confirm completely amorphous areas in FIB lift-out sections of the irradiated forsterite, olivine, and pyrrhotite, while blister skins of irradiated serpentine were amorphous.

Diffusion rates of hydrogen in silicates and oxides with ionic bonds such as enstatite, forsterite, and olivine are much slower than the experimental duration [e.g., 6]. Thus, the implanted hydrogen may move through vacancies formed by irradiated ions and recoiled atoms, and then bubbles nucleate and grow to form the blisters due to the high pressure of the hydrogen gas [7]. On the other hand, hydrogen diffusion rates in amorphous enstatite and iron meteorite may be very rapid compared to the experimental duration [13, 14]. Hydrogen escaped from the surfaces and could not accumulate to form blisters on enstatite glass and iron meteorites.

We constrained on the threshold dose of the enstatite amorphization by hydrogen ion irradiation. The difference of the threshold doses of blister formation and amorphization, and of the blister structures indicates that we can evaluate the solar-wind irradiation age of the asteroidal regolith more quantitatively form the combination of blister and crystal structures of multiple minerals consisting one regolith.

[1] Hapke (2001) JGR, 106, E5, 10039-10073. [2] Clark B. E. et al. (2002) in Asteroid Space Weathering and Regolith Evolution, Asteroids III. pp. 585–599.. [3] Noguchi et al. (2014) MAPS, 49, 188-214. [4] Margolis et al. (1971) LPSC, 2, 909. [5] Demyk et al. (2004), A&A, 420, 233-243. [6] Stalder and Skogby (2003) PCM, 30, 12-19. [7] Muto and Enomoto (2005), Materials Trans., 46, 2117-2124. [8] Shang et al. (2009) GCA, 73, 5435-5443. [9] Hagi, Hayashi, and Ohtani (1978) J. Japan Inst. Metals, 8, 801-807.

Keywords: space weathering, asteroid, ion irradiation

Irradiation experiments on CM chondrites: To estimate surface textures of the returned samples by Hayabusa 2

*Takaaki Noguchi[1], Yuji Miyake[2], Ryuji Okazaki[2], Takahito Osawa[3], Hiroyuki Serizawa[3], Hikaru Yabuta[4], Tomoki Nakamura[5]

1. Faculty of Arts and Science, Kyushu University, 2. Department of Earth and Planetary Science, Kyushu University, 3. Japan Atomic Energy Agency, 4. Department of Earth and Planetary System Science, Hiroshima University, 5. Department of Earth Sciences, Tohoku University

Introduction: In 2020, Hayabusa 2 spacecraft will return the surface and sub-surface samples from the asteroid (162173) Ryugu, a C-type asteroid. We will have an opportunity to investigate pristine materials from a C-type asteroid. Because CM chondrites contain solar gases and because most of they contain abundant subangular mineral and lithic fragments, they are regolith breccias (e.g. [1], [2], [3] and references therein). Although solar noble gases are restricted to the clastic matrix [1], [2], textures related to the solar wind irradiation and/or micrometeoroid impacts have not been identified among CM chondrites. Although there are many spectroscopic studies of CM chondrites (e.g. [4]), only a few studies are focused on the textural changes related to the micrometeoroid impacts and solar wind irradiation on CM chondrites (e.g. [5], [6]). In this study, we performed spectrum measurements, micro-petrographic study, and C Kα X-ray absorption near-edge structure measurement of irradiated CM chondrites. These studies will serve to understand the space weathering on the surface of fine-grained Ryugu grains because it is highly likely that space weathering will be found on the surface of Ryugu grains.

Samples and methods: We performed irradiation of 4 keV He^+ ions on Murchison CM chondrites at Takasaki Advanced Radiation Research Institute, Japan Atomic Energy Agency (TARRI, JAEA). The fluences are 5 $\times 10^{16}$ and 5 $\times 10^{17}$ He^+/cm^2, which correspond to ~10^2- and ~10^3-year irradiation at 1.1 AU (the averaged orbital radius of Ryugu). Reflectance spectra of the irradiated surface were measured at JASCO Co. Ltd. by using JASCO V-670 absorption spectrometer with an integrating sphere. The irradiated samples were observed by field-emission scanning electron microscope (FE-SEM) at JAEA and Kyushu University. We observed the samples by using 2 or 3 kV acceleration voltage to avoid structural changes during observation. Thin samples were prepared by using scanning electron microscope-focused ion beam sample preparation machine and low acceleration voltage Ar milling machine at Kyushu University. They were observed by transmission electron microscope (TEM) at Kyushu University.

Results and discussion: Reflectance spectrum of the sample irradiated by a fluence of 5 $\times 10^{16}$ He^+ does not show remarkable difference from the spectra of an un-irradiated sample. By contrast, a broad absorption from 0.7 to 1.4 μm, related to the absorption by Fe-rich serpentine group minerals, is disappeared in the case of the sample irradiated with 5 $\times 10^{17}$ He^+. These data suggest that 1000-year equivalent solar wind irradiation gives an effect on the shape of reflectance spectra, which is similar to the effect by dehydration [4]. There is no remarkable difference in surface morphology of the sample irradiated by a fluence of 5 $\times 10^{16}$ He^+ from those of un-irradiated sample. On the other hand, the sample irradiated with 5 $\times 10^{17}$ He^+ shows blistering on both matrix and chondrules. The surface of fine-grained matrix has a ~30-nm thick amorphous layer. In the amorphous layer, a small amount of nanoparticles is observed. Their 0.2-nm lattice fringes suggest that they are nanophase Fe^0. In the case of the sample irradiated with 10^{17} He^+ has ~60-nm amorphous rim containing abundant bubbles (blistering), which is especially remarkable in cronstedtite-tochilinite intergrowth. Just below the amorphous layer, both cronstedtite and tochilinite show sharp lattice fringes. The amorphous rim contains abundant nanoparticles is observed. They also show 0.2-nm lattice fringes, suggestive of nanophase Fe^0. This result is consistent with [5].

References: [1] Nakamura T. et al. (1999a) GCA 63, 241-255. [2] Nakamura T. et al. (1999b) GCA 63, 257-273. [3] Krot A. et al. In: Meteorites and the early solar system II, pp. 679-712. [4] Hiroi T. et al. (1993) Science 261, 1016-1018. [5] Matsuoka M. et al. (2015) Icarus 254, 135-143. [5] Keller L. P. et al. (2015) LPSC 46, Abstract #1913.

Keywords: irradiation experiment, CM chondrites, TEM

Abrasion experiments of quartz particles simulating the regolith abrasion on airless bodies: change in their 3D shapes

*Motohiro Ogawa[1], Akira Tsuchiyama[1], Tokiyuki Kadokawa[1], Takushi Sakurama[1], Tsukasa Nakano[2], Kentaro Uesugi[3]

1. Division of Earth and Planetary Sciences, Graduate School of Sciece, Kyoto University, 2. Geological Survey of Japan, AIST, 3. SPring-8/JASRI

Some of Itokawa and lunar regolith particles have rounded edges and mechanical abrasion was proposed for these particles [1,2]. Particles should rub against each other on a body without fluids by particle motion. On Itokawa, seismic wave induced by micro-meteoroid impacts [1], YORP effect and tidal motion [3] were proposed for the abrasion process. In this study, we made abrasion experiments in order to understand how the shapes of particles and their edges change in 3D.
The experiments were made using quartz particles with a mill (Multi-beads-shocker: YASUIKIKAI Co.). We chose quartz because the strength is similar to olivine and pyroxene although it is almost absent in meteorites and moon samples and also because a large amount of the sample is available. Single crystals of colorless quartz were crushed in a tungsten carbide mortar, and particles 1-2 mm in size were selected with sieve. These particles (~6.5g) were put into an agate vessel (10 mL) with ~50% fraction without any crushing tool. Then the vessel was rotated together with the vertically-vibrational motion.
Two types of experiments were performed. In the first type of experiments (Exp-1), the samples were rotated at a rate of 1500 or 2500 rpm for durations of 5, 30, 120 and 180 min. In each run, powder (<250 μm) produced by abrasion was collected with sieve, and the mass of the powder was calculated from the difference between the particle mass before and after the run. More than 150 particles randomly sampled were imaged by X-ray CT at Tohoku University (X-ray tube voltage140 kV, pixel size: 14.5 μm) to obtain their 3D shapes. In second type of experiments (Exp-2), three kinds of colored quartz crystals (amethyst, citrine and morion) were crushed and two particles (1-2 mm) of each (totally six particles) were mixed with colorless quartz particles. The samples were abraded at a rate of 1500 or 2500 rpm for accumulated durations of 1, 5, 10, 30, 60, 120 and 180 min. After each abrasion cycle, the colored particles were picked up and their 3D shapes were imaged using X-ray CT system at BL20B2 of SPring-8 (25keV, pixel size: 2.75 μm). After the imaging, the particles were cleaned and returned to the agate vessel, and the abrasion cycles were repeated.
The volume, *V*, surface area, *S*, and 3-axial lengths of each particle were obtained from the CT images. Then, we calculated the 3-axial ratio, angularity (*V* of approximated ovoid/*V*) and sphericity (*S*/*S* corresponding to approximated ovoid). In Exp-2, 3D models of colored particles after each abrasion cycle were made for examining change in their 3D shapes.
The powder mass produced by abrasion and sphericity increased while *V*, *S* and angularity decreased with time in Exp-1 and -2. Changing rates of these parameters were larger at 2500 rpm than 1500 rpm except for sphericity, and the changing rates largely decreased in the initial 30 min. In Exp-1, the average 3-axial ratio was almost unchanged with time at 1500 rpm while it increased at 2500 rpm (the particle shape became equant). In Exp-2, the 3-axial ratios of the colored particles differently changed grain by grain suggesting that the behavior of the 3D-axial ratio observed in Exp-1 should occur as a total behavior of individual particles.
Changes in the colored particle shapes showed that abrasion advanced by chipping particle edges at 2500 rpm while by gradual wearing almost without chipping at 1500 rpm. The present results on the difference by the rotation rates can be explained by these two abrasion modes. Comparison with Itokawa and lunar regolith particle shapes may suggest that Itokawa particles only experienced light abrasion

without chipping while lunar particles experienced heavy abrasion with chipping as discuss in more detail in [4].
[1] Tsuchiyama et al. (2011) *Science*, 333: 1121. [2] Tsuchiyama et al. (2016) 4th *Symp. Solar System Materials*, abstr. [3] Connolly et al. (2015) *EPS*, 67: 12. [4] Tsuchiyama et al. (2017) *JpGU*, abstr.

Keywords: Itokawa, lunar, abrasion

Detection of CME components of solar wind noble gas from DOS sample of *Genesis*

*Azusa Tonotani[1], Ken-ichi Bajo[1], Chad T Olinger[2], Amy J G Jurewicz[3], Isao Sakaguchi[4], Taku Suzuki[4], Donald S Burnett[5], Satoru Itose[6], Morio Ishihara[7], Kiichiro Uchino[8], Hisayoshi Yurimoto[1,9]

1. Hokkaido University, 2. Los Alamos National Laboratory, 3. Arizona State University, 4. National Institute for Materials Science, 5. California Institute of Technology, 6. JEOL Ltd, 7. Osaka University, 8. Kyusyu University, 9. JAXA

Introduction: Noble gases in solar wind (SW) can be utilized as a tracer to investigate solar activity from the SW irradiated materials. Recently, *Genesis* spacecraft mission by NASA was carried out in order to determine the composition of the Sun and estimate that of the solar nebula. *Genesis*-returned sample was measured, and the energy distribution, flux of the SW, and isotopic and elemental composition of the SW noble gases are well determined by in-situ measurements (e.g. Heber et al., 2009; 2012). In order to discuss the solar activity, an interaction between the implanted SW and the substrate (ion-solid interaction) is important issue. A depth profile of the implanted particles into the substrate is correlated with the energy distribution of SW particles. However, depth profiling of noble gases was not established because (1) an implant depth of SW noble gases is much shallower than 1 μm and (2) a conventional depth profiling with secondary ion mass spectrum (SIMS) was hard to measure noble gases because of their high ionization potentials.
Recently, Laser ionization mass nanoscope (LIMAS) was developed to measure depth profiles for noble gases (Bajo et al., 2015).
LIMAS is a type of the secondary neutral mass spectrometer with strong-field photoionization (Laser power density: ~10^{20} W m^{-2}). LIMAS consists of a Ga liquid metal ion source and an aberration corrector for sputtering of nanometer scale area on samples, a femtosecond laser for tunneling-ionization of the sputtered neutrals, and a multi-turn time-of-flight mass spectrometer (MULTUM II) for isotope analysis (Ebata et al., 2012; Bajo et al., 2015).
Bajo et al. (2015) carried out depth profiling in the *Genesis* sample by using LIMAS. However, the ^{4}He concentration of sample deeper than 120 nm from the surface, corresponding to the implanted depth of CME particles, was equivalent to the residual He gas amount of 3 ×10^{18} atoms cm^{-3} in sample chamber of LIMAS. Therefore, the ^{4}He depth distribution of deep area (>120 nm) in *Genesis* sample has not been determined. In this study, we improved the method for the high precision depth profile of SW noble gases.
Experimental procedure: A diamond-like carbon-film on silicon substrate (DOS) sample of *Genesis* was prepared in this study.
LIMAS was used for the measurement of depth profile of SW. A pulsed primary beam of 1.5 μm in diameter with ~50 nA was used. The newly installed fs-laser with pulse energy was 5.6 mJ at the repetition rate of 1 kHz. Setting of the mass spectrometry of LIMAS was based on Tonotani et al. (2016).
Multi-turning of ^{4}He ions was set to 100 cycles and ion gates were used for the elimination of interfering ion such as $^{12}C^{3+}$. To reduce residual gases in sample chamber of LIMAS, we exchanged sputter ion pumps and added getter pumps. Raster area in *Genesis* sample for depth profile was set to 20 ×30 μm. After depth profiling, atomic force microscope (Asylum Technology, MFP-3D-BIO-J) was used for the measurement of crater shapes.
Results and discussion: ^{4}He background in this study was reduced to 4 ×10^{17} atoms cm^{-3} for DOS sample, which is one order of magnitude lower than that of Bajo et al. (2015) (i.e. 3 ×10^{18} atoms cm^{-3}). As a result, Depth profile of SW He was traced to the depth of 300 nm from surface. The profile deeper than 100 nm corresponds to CME components. Moreover, depth profile for SW ^{20}Ne was determined from the DOS

sample.

Keywords: Genesis, Solar wind, Noble gas, CME, SNMS, Depth profile

Time-resolved analysis of shock-driven structure transformation of forsterite single crystals using power laser and x-ray free electron laser

*Takuo Okuchi[1], Narangoo Purevjav[1], Norimasa Ozaki[2], Yusuke Seto[3], Yoshinori Tange[4], Toshimori Sekine[5], Takeshi Matsuoka[6], Kenjiro Takahashi[6], Yuichi Inubushi[4], Makina Yabashi[7], Kazuo Tanaka[2], Ryosuke Kodama[2,6]

1. Institute for Planetary Materials, Okatama Univ., 2. Faculty of Engineering, Osaka Univ., 3. Faculty of Science, Kobe Univ., 4. JASRI/SPring-8, 5. Faculty of Science, Hiroshima Univ., 6. Photon Pioneers Center, Osaka Univ., 7. RIKEN SPring-8 Center

We analysed time-resolved structure evolution of shock-compressed single crystals of forsterite using power laser and x-ray free electron laser at SACLA, SPring-8. It was indicated from these results that forsterite structure (orthorhombic) transforms into ringwoodite structure (cubic spinel) in very fast time scale of few nanoseconds, which has implication on the origin of ringwoodite observed in meteorites.

Keywords: forsterite, ringwoodite, x-ray free electron laser , laser-driven shock compression, high-speed collision

Nanometer-scale paleomagnetism of meteorites using electron holography

*Yuki Kimura[1], Kazuo Yamamoto[2]

1. Institute of Low Temperature Science, Hokkaido University, 2. Japan Fine Ceramics Center

Remanent magnetization of minerals is very sensitive to the formation and experienced environments such as temperature and magnetic field. To better understand the formation environments of individual extraterrestrial minerals, we attempted to apply the electron holography to nanoparticles extracting from a meteorite. As the result, we succeeded to elucidate a magnetic structure of framboidal magnetite, which has been aligned periodically in three-dimensionally and proposed its formation process in a parent body of the Tagish Lake meteorite [1]. This method will allow us to reveal formation temperature of individual tiny minerals in the solar nebula and precipitation temperature of individual minerals during thermal aqueous alteration inside a corresponding asteroid. More resent years, several reports about paleomagnetic studies of meteorites has been reported [e.g. 2]. Here, we will show our present approaches to visualize the magnetic structures of individual extraterrestrial minerals and to constrain its formation environment, which was not unveiled by conventional paleomagnetic studies using a bulk mineral.

[1] Yuki Kimura et al., Nature Communications, 4 (2013) 2649.

[2] J. Bryson, et al., Earth and Planetary Science Letters, 388 (2014) 237.

Acknowledgment: This work was supported by a Grant-in-Aid for Challenging Exploratory Research from KAKENHI (16K13909).

Keywords: Electron holography, Remanent magnetization, Transmission electron microscopy, Tagish Lake meteorite, Magnetite, Aqueous alteration

Properties of submicron craters on Itokawa regolith particles

*Toru Matsumoto[1], Sunao Hasegawa[1], Hisayoshi Yurimoto[1,2]

1. Institute of Space and Astronautical Science, 2. Hokkaido University

Introduction: The Hayabusa spacecraft recovered surface regolith particles from S-type asteroid Itokawa. Micrometeoroid impacts are considered to be among the important agents for surface modification processes on Itokawa such as dynamic regolith mixing/convection and space weathering. In previous studies, submicron sized craters have been reported on Itokawa particles [1, 2, 3]. The craters are expected to have been formed through the impacts of secondary ejecta created by primary impacts on Itokawa [2, 3]. Since only 24 craters have been reported on Itokawa particles so far [1, 2, 3], statistical analysis of the craters is limited. In this study, we performed extensive investigations of submicron craters on Itokawa particles. The purpose of this work is the detailed characterization of abundance, areal and size distributions, and morphologies of submicron craters.
Experiment: We investigated 34 Itokawa regolith particles from approximately 10 μm up to 200 μm in size. We observed the surface morphology of the Itokawa particles using a scanning electron microscope (SEM; Hitachi SU6600). Secondary electron (SE) imaging was conducted at an accelerating voltage of 2 kV in high vacuum.
Results and Discussion : We found 8 Itokawa particles over 80 μm in size, with surfaces with numerous submicron craters. Such crater-rich particles account for approximately 40 % of Itokawa particles over 80 μm in size observed in this study. In this study, we identified craters ranging from approximately 10 nm to 700 nm in diameter. The morphologies of the craters are similar to those of microcraters on lunar regolith [4]. From the size distribution and areal density of more than 400 craters on 3 Itokawa particles, we estimated the flux of impactors that formed submicron craters. We assumed that the craters accumulated during direct exposure to space for 10^3 years from the common appearance of blisters on the surface. We compared impactor flux on Itokawa regolith with impactor flux on the lunar surface [4] and interplanetary dust flux models [5]. The comparison revealed that the flux on Itokawa particles is up to two orders of magnitude higher than the interplanetary dust flux and is also comparable to the case of the Moon. Higher lunar and Itokawa surface flux over interplanetary flux can be explained by high-speed secondary ejecta impacts and not by primary meteoroid impacts [10]. Secondary impacts will have significant effects for submicron-scale cratering on airless bodies of various sizes in the solar system.
References: [1] Nakamura et al. (2012) *PNAS, 109*, E624-E629. [2] Matsumoto et al. (2016) *GCA, 187,* 195-217. [3] Harries et al. (2016) *EPSL, 450,* 337-345. [4] Morrison and Clanton (1979) *LPS X*, Abstract pp.1649-1663. [5] Jehn (2000). *Planet. Space Sci., 48*, 1429–1435.

Keywords: Regolith, Asteroid Itokawa, Crater

Application of an X-ray diffraction method to polished thin section of CO3 chondrites: Mineralogy and thermal history

*Naoya Imae[1,3], Yoshihiro Nakamuta[2]

1. Antarctic Meteorite Research Center, National Institute of Polar Research, 2. Kyushu University Museum, Kyushu University, 3. SOKENDAI

Introduction
The X-ray diffraction method is useful for the characterization of stony meteorites, which is independent of the characterization determined by the combination of the observation under an optical microscope and variations of Fa# and Fs# by EPMA. This method enables to obtain the quantitative data as well as to obtain the consistent result with the canonical method. In the present study, CO3 chondrites were examined on mineralogy and the thermal history, using the method.
Studying method
The X-ray diffractometor, SmartLab (RIGAKU), was used for the study. The incident X-ray, CuKa generated from with tube voltage 40 kV and tube current 30 mA, irradiated to the rotating polished thin section in plane through the slit of 10mm square. Ten CO3 chondrites were used, which are shown in the following with the subtype: ALH77307 3.03, Y81020 3.05, Colony 3.0, A881632 3.1, Y983589 3.4, Lance 3.5, A882094 3.5, Y791717 3.5, ALH77003 3.6, and Isna 3.8.
Results and Discussion
The olivine (130) peak is single more than 3.8 subtype, but is splitted less than 3.6, corresponding to ferroan olivine in matrices at lower 2 theta and magnesian olivine in chondrules at higher 2 theta. The subtype clearly correlates with the full width of half maximum of the peak(s). It also correlates with the integrated intensity ratio of the splitted peak, but the subtype 3.0 has exceptionally high Mg/Fe, consistent with the report of amorphous Fe-silicates in matrices in 3.0 (Howard et al., 2014; Bonato et al., 2016). The relative intensity ratio (I_{Mg}/I_{Fe}) except 3.0 can connect with volume ratio (V_{Mg}/V_{Fe}) using the olivine grain size (50 μm in diameter) and ferroan olivine growth with thickness, d, where d implies the mean diffusion length due to the Fe-Mg volume diffusion in olivine during the cooling on the parent body. Also considering the inhibited Mg-Fe diffusion of clinoenstatite, the peak temperature in the parent body is obtained to be 620-900K, which is consistent with the estimation by Schwinger et al. (2016). In addition, the modal abundance for the amorphous Fe-silicate of CO3.0 is estimated to be 11-22%, nearly consistent with those of Bonato et al. (2016) and Howard et al. (2014).
References
Bonato E. et al. 2016. 79th Ann. Meeting. Met. Soc. #6466.
Howard K. T. et al. 2014. 45th LPSC #1830.
Schwinger S. et al. 2016. GCA, 191, 255.

Keywords: CO3 chondrites, mineralogy, thermal history , X-ray diffraction method, amorphous silicates

4D in situ observation of formation process of chondrules

*Masayuki Uesugi[1], Kentaro Uesugi[1], Masato Hoshino[1]

1. Japan synchrotron radiation research institute

Chondrule is tiny rocky spherules around 1mm in diameter, and constitutes a large volume of chondrite which dominates more than 80% of meteorites fallen onto the Earth. Dating studies using radiogenic nuclides have showed that they were formed in very early stage of the solar nebula evolution, and thus would show the important step of the evolution of solid materials which formed rocky planets, i.e. terrestrial planets and asteroids.
Their shape clearly indicates that they were solidified from molten droplets. However, the formation process of them, such as heat source and thermal history, precursor material, formation region in the early solar nebula, are still unknown.
In previous studies, several heating experiments for the reproduction of their characteristic textures were conducted. However, complete reproduction of their textures has not been succeeded yet. One of the difficulties is that growth process of crystals inside the chondrules is difficult to observe. Silicate materials melted above 2000K emits strong radiation. In this situation, phenomenon occurred inside a few mm sample is difficult to observe with high spatial resolution by visible light.
In this study, we developed a new devise for in situ 4D observation, 4D means 3D + time elapse, of crystallization process of chondrules using synchrotron radiation computed tomography, and conducted heating experiments of analog materials. We show preliminary result of the experiments, and discuss the problems of heating experiments of previous studies based on the results obtained by our new setup. We will also show future plan for our investigation, and also show the possible heating experiment for the chondrule formation using the system.

Keywords: chondrules, in situ observation heating experiment, 4D-CT

Three-dimensional structure of matrix of the Ivuna meteorite using micro X-ray CT and FIB serial sectioning

*Akira Kitayama[1], Akira Tsuchiyama[1], Akira Miyake[1], Tsukasa Nakano[2], Kentaro Uesugi[3], Akihisa Takeuchi[3], Akiko Takayama[1], Shoichi Itoh[1]

1. Kyoto University, 2. AIST, 3. SPring-8 / JASRI

CI chondrites are chemically the most primitive material in the solar system because of their bulk composition similar to the solar photosphere except for volatiles [1]. They have undergone extremely strong aqueous alteration. Their matrices mainly consist of phyllosilicates and include mineral grains such as magnetite, sulfides, carbonates and sulfates. Two types of phyllosilicates are known; coarse aggregates of serpentine and saponite and fine aggregates of serpentine, saponite and ferryhydrite [2]. CI chondrites are composed of rock fragments with different lithologies. Four lithologies were identified for the Ivuna meteorite based on the mineral composition using SEM [3]. Fragments of four CI chondrites were classified into eight lithologies based on the textures and the chemical compositions of the matrices using SEM and TOF-SIMS, and a model for aqueous alteration and accumulation was proposed [4]. Each lithology has fine and complex texture. Detailed 3D structures enable us to obtain information such as cavity, which is not available in 2D. From the information, we may understand original state before aqueous alteration, detail process of aqueous alteration such as movement of a fluid. For this purpose, we observed 3D structure of a fragment of the Ivuna meteorite with high resolution using X-ray tomography and FIB serial sectioning.

We made detailed observation of fragments in a thin section of the Ivuna meteorite and obtained elemental maps with FE-SEM/EDX (JEOL JSM7001F/Oxford Instruments X-Max^N 150mm^2). Based on the result, a cube ~25 μm in size was sampled from one of the fragments using SEM/FIB (FEI Helios NanoLab G3). Then, the 3D structure of the cube sample was imaged by SIXM (Scanning Imaging X-ray Microscopy) [5] at BL47XU of SPring-8, Japan with the pixel size ~100 nm. After the CT imaging, we obtained serial BSE images of some portion of the sample with higher resolution by serial sectioning using FIB and observation with FE-SEM (FEI Helios NanoLab G3). From these 3D images, structures in the matrix and mineral grains were extracted using image analysis.

The SEM/EDX study of the thin section showed that the fragment examined in 3D has Mg-rich matrix mainly consisting of coarse and elongated phyllosilicate aggregates (~50 nm in width and ~500 nm in length). Mineral grains of magnetite, pyrrhotite and Ni bearing sulfates were also observed, but any carbonates were not. These features correspond to lithology II (carbonates are absent but sulfates are dominant) of [3] and lithology CGA (Coarse-grained phyllosilicate aggregate) of [4]. We found that the matrix consists of objects a few mm in size, which are aggregates of Mg-rich phyllosilicates covered with Fe-rich phyllosilicate and seem to be spherical in 2D. Hereafter, we call this object PC (phyllosilicate composite).

In the CT images, rod-shaped crystals of magnetite (~1×5 μm) and cavities in irregular and hexagonal-plate shapes were observed as well as PC. Cavities in hexagonal shape (~5×1 μm) should be empty crystals formed by leaching of original pyrrhotite or carbonate. In the serial SEM images, PCs and magnetite crystals was clearly recognized, but cavities not because spattered substances by FIB were redeposited in the cavities. We found that PCs are irregular ellipsoids in 3D, and the directions of elongations of PCs and magnetite crystals are random, suggesting that no remarkable movement of a fluid was occurred during aqueous alteration. Matrix texture consisting of PCs might be a result of strong aqueous alteration of fine aggregates of sub-micron grains of minerals and/or amorphous silicate.

[1] Anders and Grevesse (1989) *GCA*, 53: 197-214. [2] Tomeoka and Buseck (1988) *GCA*, 52: 1627-1640. [3] Endreβ and Bischoff (1993) *MAPS*, 28: 345 (abstr.). [4] Morlok et al. (2006) *GCA*, 70: 5371-5394. [5] Takeuchi et al. (2013) *J. Synchrotron Rad.,* 20: 793–80.

Keywords: CI meteorite, aqueous alteration

3D structure of primitive carbonaceous chondrite Acfer 094: investigation of amorphous silicates

Aiko Nakato[1], *Akira Tsuchiyama[1], Megumi Matsumoto[2], Junya Matsuno[1], Akira Miyake[1], Kentaro Uesugi[4], Akihisa Takeuchi[4], Tsukasa Nakano[5], Epifanio Vaccaro[3], Sarah Russell[3]

1. Kyoto University, Division of Earth and Planetary Sciences, 2. Kobe University, Center for Supports to Research and Education Activities, 3. National History Museum, London, 4. Japan synchrotron radiation research institute, 5. AIST, Geological Survey of Japan

Introduction: Amorphous silicates known as a major constituent material in chondritic porous (CP-) IDPs are one of the most primitive materials in the solar system. However, amorphous silicates in the meteorites are rarely observed [e.g., 1, 2, 3], and the relationship with that in CP-IDPs has not been clarified yet. Acfer 094 is recognized as one of the most primitive carbonaceous chondrites, since it includes abundant presolar grains and minor hydrous minerals [e.g., 1, 4, 5]. In addition, some researchers reported that Acfer 094 is one of the unique meteorites that contains much amorphous silicates in the matrix [1, 2]. We have focused on the 3D structure of textures including amorphous silicates in Acfer 094 matrix to understand the origin, the earliest stage of accretion and aqueous alteration processes in the solar system.

Methods: FE-SEM observation was carried out on approximately 1x2 mm polished section for understanding the heterogeneity of the sample. Based on the obtained EDS/BSE-map, we selected some areas and fibbed about 25x25x30 μm for nondestructive Synchrotron radiation (SR)-based X-ray computed tomography (SR-XCT). We obtained 3D structures of the samples with the voxel size of ~100 nm by using SR-XCT at SPring-8 BL47XU in Japan. A method using absorption contrasts called "dual-energy tomography" (DET) to obtain 3D distribution of minerals [6], a newly developed technique using phase and absorption contrasts called "scanning-imaging x-ray microscopy" (SIXM) to discriminate between void, water and organic materials [7], and their combined analysis [8] were applied to all fibbed samples.

Results and Discussion: FE-SEM observation revealed that the matrix shows rather homogeneous texture and chemical composition. In addition, we found some unique phase that are similar to cosmic symplectite (COS) in the texture and chemical composition [8]. Typical COS is only observed in Acfer 094 matrix, and shows very heavy oxygen isotopes [8]. We expected that COS can be a good indicator of the primitive area including amorphous silicates in the Acfer 094 matrix, since the unique isotopes should be changed easily by thermal and/or aqueous alteration on the parent body. Thus, we picked up 2 samples, one is from the area having COS and another is from the representative matrix area, using FIB for SR-XCT. Based on the SR-XCT observations, we identified several lithologies having different porosity and texture within both sample. A lithology (lith4) showing low porosity and fibrous minerals as same as aqueous alteration product, and another lithology (lith1) showing extensively high porosity are complexly mixed. The lith1 (10-20 μm in size) distributes throughout the matrix and shows distinct boundary between other lithologies. According to DET analysis obtained by SR-XCT, the estimated texture and chemical composition of the lith1 is similar to that of CP-IDP. It suggests that lith1 mainly consists of amorphous silicates. We will present the results including detailed TEM observation of lith1, and discuss the relationship between each lithology, the primitiveness, and presence or absence of amorphous silicates.

References: [1] Greshake, 1997, *Geochimica et Cosmochimica Acta,* 61, 437-452. [2] Balnd et al., 2007, *Meteoritics & Planetary Sciences*, 42, 1417-1427. [3] Leroux et al., 2015, *Geochimica et Cosmochimica Acta,* 170, 247-265. [4] Nagashima et al., 2004, *Nature*, 428, 921-924. [5] Nguyen and Zinner, 2004,

Science, 303, 1496-1499. [6] Tsuchiyama A. et al., 2013, *Geochimica et Cosmochimica Acta,* 116, 5-16. [7] Takeuchi A. et al., 2013, *J. Synch. Rad.* 20, 793. [8] Tsuchiyama et al., 2017, 48th LPSC, 2680. [9] Sakamoto et al., 2007, *Science*, 317, 231-232.

Keywords: amorphous silicate, GEMS, carbonaceous chondrite, Acfer 094

Melting and quench experiment of iron sulfide fine particles at atmospheric entry

Kento Murozono[2], *Hiroshi Isobe[1]

1. Department of Earth and Environmental Sciences, Faculty of Advanced Science and Technology, Kumamoto University, 2. Faculty of Science, Kumamoto University

Micrometeorites have the most abundant flux in current accumulation of planetary materials to the Earth. Composition and texture of micrometeorites are results of heating processes at atmospheric entry. Evaporation of meteoritic materials may have environmental effect at upper atmosphere. Troilite is typical FeS phase in chondritic meteorites. In this study, quick heating and cooling experiments of FeS reagent particles were carried out with a fine particles free falling apparatus with controlled gas flow (Isobe and Gondo, 2013). Starting material reagent is composed of troilite, mixture of Fe oxide and sulfide and iron metal. Oxygen fugacity was controlled to FMQ +1.5 log unit. Maximum temperature of the particles was higher than 1400˚C for approximately 0.5 seconds.

Run products with rounded shape and smooth surface show that the particles were completely melted. Chemical compositions of particles analyzed on cross sections are generally well homogenized from heterogeneous starting materials by complete melting. Molar ratios of Fe in melted regions are close to 0.5, while compositions of S and O are various. Varieties of S and O compositions show various degree of oxidation and evaporation of sulfur. Distribution of compositions of melted regions in Fe-S-O system is plotted in liquidus compositions of FeO and FeS saturated melt. Compositions of FeS melt in fine spherules are following Fe-S-O phase relations even in a few seconds. Evaporation of sulfur from meteoritic materials in atmospheric entry heating may depend on oxygen fugacity of the upper atmosphere. Sulfur supply from meteoritic materials to atmosphere may be limited on planets with oxygen-free atmosphere.

Keywords: troilite, micro meteorit, Fe-S-O system, magnetite, atmospheric heating

Interior structure of Mars estimated from elastic properties of liquid Fe-Ni-S

*Hidenori Terasaki[1], Yuta Shimoyama[1], Mayumi Maki[1], Fuyuka Kurokawa[1], Satoru Urakawa[2], Keisuke Nishida[3], Ryunosuke Saito[1], Yusaku Takubo[1], Yuki Shibazaki[4], Tatsuya Sakamaki[4], Akihiko Machida[5], Yuji Higo[6], Tadashi Kondo[1]

1. Graduate School of Science, Osaka University, 2. Graduate School of Natural Science and technology, Okayama University, 3. Graduate School of Science, The University of Tokyo, 4. Graduate School of Science, Tohoku University, 5. Natural Institutes for Quantum and Radiological Science and Technology, 6. Japan Synchrotron Radiation Research Institute

To give a constraint core composition and interior structures of terrestrial planets, elastic properties, such as sound velocity and density, of liquid Fe-light element alloys at high pressure are required together with geodesy observations. In this study, we have measured sound velocity and density of liquid Fe-Ni-S (S=17-30 at%) using ultrasonic pulse-echo and X-ray absorption methods combined with multianvil apparatus up to 14 GPa and studied the effects of pressure and sulfur content on the elastic properties. Measured sound velocity (V_P) of liquid Fe-Ni-S increased non-linearly with pressure and its pressure dependence is well fitted by the Birch-Murnaghan equation of state. Obtained bulk modulus of liquid Fe-Ni-S decreases with increasing sulfur content. Based on these obtained properties, we will discuss estimated radius and sulfur content of Martian core by comparison with observed moment of inertia data of Mars.

Keywords: Mars, Core, liquid, sound velocity, density

Microstructure of olivine in basalt recovered from shock experiment and a comparison with olivine in Martian meteorites

*Atsushi Takenouchi[1], Takashi Mikouchi[1], Takamichi Kobayashi[2], Akira Yamaguchi[3]

1. Department of Earth and Planetary Science, Graduate School of Science, The University of Tokyo, 2. National Institute for Materials Science, 3. National Institute of Polar Research

Martian meteorites are known to contain brown colored olivine (brown olivine) whose color is induced by iron nano-particles (Fe-nps) formed by a shock event. Brown olivine is only reported in Martian meteorites. Several previous studies discussed its formation processes (e.g., Treiman et al., 2007) although it is still in controversy. The formation processes and formation conditions of brown olivine should be quantitatively studied because they are important for understanding impact events and origins of Martian meteorites. In this study, we performed shock-recovery experiments to constrain the formation processes and formation conditions of brown olivine. In previous studies of shock-recovery experiments focusing on olivine, olivine single phase was chosen. However, rocks similar to Martian meteorites should be used as starting materials to compare shock effects on olivine. Therefore, we used olivine-phyric basalt from Kita-Matsuura, Nagasaki as a target sample. Due to the presence of Fe-rich olivine (~Fo69), this basalt is similar to Martian meteorites, particularly olivine-phyric shergottites.
The experiments were conducted using a single stage propellant gun at NIMS. The basalt chips were cut as circular disks of 1 mm thick and packed in tightly sealed stainless containers. Stainless flyers of 3 mm thick and tungsten flyer of 2 mm thick were used for ~40 GPa and 50 GPa shock, respectively. We performed four shots and actual shock pressures calculated with the flyer velocity just before the impact were 22.2, 28.7, 39.5 and 48.5 GPa. Polished thin sections (PTSs) of the recovered samples were observed by optical and scanning electron microscopy (SEM). Thin film section for TEM observation was cut off from PTS by FIB. Regarding olivine darkening, we checked the presence of Fe-np because it is difficult to judge whether olivine is darkened or not by optical microscopy because part of olivine was originally colored due to alteration.
In our observation, plagioclase shocked at 22.2 GPa showed wavy extinction while that in basalt shocked over 28.7 GPa was completely maskelynitized. Pyroxene and olivine show only wavy extinction and weak mosaicism even in basalt shocked at 48.5 GPa. Although shock melt veins formed in basalt were subjected to over 28.7 GPa, no high-pressure phases were found. Interestingly, olivine shocked at 39.5 GPa and 48.5 GPa exhibited lamellar textures similar to planar deformation features and widths of lamellae were ~0.25 and ~ 1 μm, respectively. Observation of these lamellae by TEM revealed that the lamellae corresponded to defect-rich areas. However, Fe-nps were not found even in these areas.
Our previous study revealed that brown olivine areas were composed of lamellae in Northwest Africa 1950 (Takenouchi et al., 2015). The lamellar texture observed in this study is similar to its texture, however, contains no Fe-nps and showed no characteristic features of brown olivine. Mikouchi et al. (2011) reported that the shock recovery experiments of olivine powder at 40 GPa produced Fe-nps in olivine. It is indicated that not only high-pressure but also high-temperature is needed to produce Fe-nps because powdered sample is likely to be experienced higher temperature during experiment due to its higher porosity compared to basalt. As a result, our experiments suggests that olivine darkening is occurred by formation of defect-rich lamellar texture by high-pressure followed by diffusion of iron forming nano-particles at high temperature.
The lamellar texture has a potential to be an indicator of shock pressure because the widths of lamellae change depending on the shock pressure. The lamellar width in olivine in Martian meteorites is about ~2 μm, which is similar to those in the recovered sample shocked at 48.5 GPa. On the other hand, a number

density of lamellae is higher in Martian meteorites, indicating that the shock temperature may control the number density. Thus, the lamellar texture could be an indicator of shock pressure and temperature.

Keywords: Shock-recovery experiment, Martian meteorite, Olivine

Stepwise Heating and Vacuum Crushing Analyses of Noble Gases in Martian Meteorites

*Mizuho Koike[1], Hirochika Sumino[2], Yuji Sano[1], Minoru Ozima[3]

1. Atmosphere and Ocean Research Institute, The University of Tokyo, 2. Department of Basic Science, Graduate School of Arts and Sciences, The University of Tokyo, 3. Department of Earth and Planetary Science, Graduate School of Science, The University of Tokyo

Introduction: Martian meteorites are valuable and possibly sole direct samples from Mars until future sample-return. Trapped noble gases in the meteorites are important, because they can provide not only strong evidence of their Martian origin [1][2], but also chemical and/or isotopic evolution of Martian atmosphere. However, noble gases in the meteorites are complicated mixtures of several sources; Martian atmosphere, Martian interior, radiogenic, cosmogenic, and terrestrial air (e.g.[3]–[9]).
In order to retrieve the exact Martian atmospheric records from the meteorites, one needs to know the trapping mechanism and trapped sites of the noble gases. As the first step, we have conducted combined stepped heating and vacuum crushing of several shergottites.
Samples: Tissint and SaU 008 are olivine-phyric shergottites. Tissint, fell in Morocco in 2011, is characterized by its numerous shock-melted glasses with small bubbles (<10 μm –ca. 100 μm), which might contain Martian atmosphere [8][10]. Heating analyses of pairs of SaU008 showed the incorporation of elementally fractionated terrestrial air (EFTA) in deserts [7][9]. EFTA effects were also observed in NWA 7397, a slightly weathered poikilitic shergottite [8][11]. NWA 10441 is a recently found highly shocked and moderately weathered shergottite. It is composed of ca. 15% of shock-melted glasses with a lot of vesicles [12].
Analytical Methods: The noble gas analyses were conducted with a VG3600 at the University of Tokyo. A ca. 100–200 mg chip of the each sample was separated into two groups; one for stepped heating and the other for vacuum crushing. The former fraction was heated in steps of 400°C, 600°C, 800°C, 1000°C, 1300°C, and 1800°C. The latter fraction was crushed with 2–10 MPa hydraulic ram to extract noble gases presumably from bubbles and/or fluid inclusions. The crushed samples were then picked-up and also stepped heated for comparison. All samples and vacuum lines were baked at ca. 200°C in vacuum for overnight before the analyses.
Results & Discussion: *Neon*: Most stepped heating data showed high contributions of cosmogenic Ne, while all crushing data indicated air-like Ne. This is due to either terrestrial air or Martian atmospheric Ne. It is difficult to distinguish the two because we do not know the exact $^{20}Ne/^{22}Ne$ of Martian atmosphere, although some plausible values are estimated [9].
Argon: Middle to high temperature heating showed high $^{40}Ar/^{36}Ar$ ratios. After corrections for cosmogenic ^{36}Ar and radiogenic ^{40}Ar, the trapped $^{40}Ar/^{36}Ar$ ratios indicate significant contribution of Martian atmospheric Ar. However, all crushing data were almost identical to terrestrial Ar. This may be attributable to either (i) expected bubbles in the shock-melted glasses did not contain Martian atmosphere or (ii) the crushing was not enough to extract gases from the bubbles.
Krypton and Xenon: As similar to Ar, high temperature heating showed excesses in $^{129}Xe/^{132}Xe$ ratios, indicating significant Martian contributions. All crushing data plotted on a mixing line between terrestrial air and EFTA (or Martian interior) in a diagram of $^{84}Kr/^{132}Xe_{trapped}$ – $^{129}Xe/^{132}Xe$ ratios. These data also support the possibility of absent of Martian atmosphere in the expected bubbles.

References: [1] Owen et al (1977) *JGR* 82, 4635-4639. [2] Becker and Pepin (1984) *EPSL* 69, 225-242 [3] Ott (1988) *GCA* 52, 1937-1948. [4] Bogard and Johnson (1983) *Science* 221, 651–654. [5] Schwenzer

(2007) *MaPS* 42, 387-412. [6] Wiens (1988) *EPSL* 91, 55–65. [7] Mohapatra et al. (2009) *GCA* 73, 1505–1522. [8] Wieler et al. (2016) *MaPS* 51, 407-428. [9] Park et al. (2017) LPSC XLVIII abst#1157. [10] Chennaoui Aoudjehane et al. (2012) *Science* 338, 785-788. [11] Ruzicka et al. (2015) Meteoritical Bulletin, No. 102. [12] Meteoritical Bulletin Database, (No.104, in prep).

Keywords: Martian meteorites, noble gas isotopes, analytical cosmochemistry

The Difference Acidic Condition of Aqueous Alteration Event of Nakhla and Yamato 000593 Based on Chemical Speciation

*Hiroki Suga[1], Natsumi Sago[1], Masaaki Miyahara[1], Takuji Ohigashi[2], Yuichi Inagaki[2], Akira Yamaguchi[3], Eiji Ohtani[4]

1. Graduate School of Science, Hiroshima University, 2. UVSOR Synchrotron, Institute for Molecular Science, 3. National Institute of Polar Research, 4. Graduate School of Science, Tohoku University

Nakhlites (*e.g.,* Nakhla, Lafayette, Governador Valadares, Millar Range (MIL) 03346, and Yamato (Y) 000593) originating from the near-surface of the Mars are expected to record a water-rock reaction (alteration) occurred on the Mars. One of the representative alteration textures is “iddingsite texture”, which is observed in and around the olivine grain of nakhlites [*e.g.,* 1]. A nonstoichiometric distorted olivine-type mineral laifunite [$(Fe^{2+}Fe^{3+})_2(SiO_4)_2$], which is one of the alteration products of original olivine, was formed in the iddingsite texture [2]. The iddingsite was crosscut by fusion crust, indicating that the iddingsite including laifunite was formed on the Mars before it was delivered to the Earth [3]. A member of Nakhlites, Y 000593 and MIL 03346, which are expected to originate from the subsurface (~10 m in depth) of the Mars, has a remarkable amount of jarosite [KFe3(SO4)2(OH)6]-bearing iddingsite [2, 4]. Iron sulfates including jarosite were detected on several provinces of Mars’ s surface such as Meridiani plume, strongly suggesting the existence of surface (or sub-surface) liquid water (probably high acidic brine) at least one period in the Martian history [5, 6]. These jarosite-bearing nakhlites would become a keystone for a direct linkage between Martian meteorites and Martian surface materials. Therefore, we have tried to describe secondary minerals in the Yamoato 000593 for elucidating environment on the Mars during a wet-period by using a microscopic speciation technique; a FIB-assisted STXM combined with a TEM/STEM observation.

A polished chip sample of Y 000593 (subsample, 120) was prepared for this study. Iddingsite textures were observed using a FE-SEM/EDS first. A laser micro-Raman spectroscope was employed for phase identification. Ultra-thin sections of iddingsite textures were prepared by a FIB system for STXM and FE-TEM/STEM analyses.

Laihunite, Opal-A [$SiO_2 \cdot nH_2O$], jarosite, natrojarosite [$NaFe_3(SO_4)_2(OH)_6$], goethite [FeO(OH)], and ferrihydrite [$5Fe_2O_3\ 9H_2O$] were identified from the iddingsite of Y 000593 based FIB-assited STXM-TEM/STEM analyses subsequent to FE-SEM/EDS and Raman analyses. The presence of natrojarosite, one of the quad phase of jarosite [7], suggests that Y 000593 experienced low pH (= 1-4), low temperature (80-240 ˚C), and SO_4-rich aqueous alteration process. Iddingsite can form below 500 , and most of them were formed between 100 and 50 [8], which is consistent with the alteration temperature of Y 000593 deduced from the existence of natrojarosite. The alteration condition of Nakhala with siderite ($FeCO_3$)-bearing iddingsite texture was estimated to be about mid pH (= 6-8), low temperature (150-200), and CO_2-rich fluid [9]. Because Mars rover Opportunity detected sulfate minerals such as jarosite and natrojarosite, Y 000593 is a better sample than the other near-surface nakhlaites to understand the late-stage acid-sulfate alteration event. Laihunite (was formed at temperatures between 400-800 in [10]) was only reported from Y 000593 and MIL 03346 in the near-surface nakhlaites, implying that these two nakhalite might have experience different alteration process compared to other near-surface nakhlaites [4]. Our STXM-TEM/STEM analyses reveal the alteration process from original olivine to laihunite; Fe^{2+}/Fe^{3+} ratio gradually decreases from olivine to laihunite, which probably corresponds to the difference of superlattices of laihunite (2M and 3M phase) [11]. Short time oxidation related to formation of the 2M phase [11], suggests that Y 000593 experienced a temporary heating event. We found mismatch on the formation temperatures between natrojarosite and laihunite. The

discrepancy may indicate that these minerals were formed different alteration events; i.e., laihunite was formed before the late-stage acid-sulfate alteration event.

[1] Treiman, 2005. [2] Noguchi et al., 2009. [3] Treiman and Goodrich, 2002. [4] Hallis and Taylor, 2011. [5] Klingelhöfer et al., 2004. [6] Ehlmann et al., 2016. [7] Papike et al., 2006. [8] Treiman et al., 1993. [9] Bridges and Schwenzer, 2012. [10] Banfield et al., 1990. [11] Tomioka et al., 2012.

Keywords: Nakhlite, Yamato 000593, Iron sulfate mineral, Laihunite, Acidic aqueous alteration on the Mars, FIB-assisted STXM/TEM

Formation of silica polymorphs in non-cumulate eucrites as inferred from crystallization experiment

*Haruka Oono[1], Akira Yamaguchi[2], Atsushi Takenouchi[1], Takashi Mikouchi[1]

1. Department of Earth and Planetary Science, The University of Tokyo, 2. National Institute of Polar Research

1.Introduction

Silica minerals have 23 or more polymorphs including metastable phases under various temperature and pressure conditions (e.g., Kihara 2001). For example, tridymite has more than 10 metastable phases at below 400 °C (e.g. Graetsch and Flörke, 1991). It is also known that silica minerals are crystallized under hydrothermal environment. For example in meteorites, quartz veinlets were found in the Serra de Magé cumulate eucrite, which was interpreted to have deposited from water (Treiman et al., 2004). Therefore, silica minerals are considered to be important to understand low-temperature thermal history and possibility of secondary alteration. However, silica minerals are usually reported only as “silica” in meteorites. In our previous studies, we analyzed silica minerals in both cumulate and non-cumulate eucrites to compare their formation conditions at depth and surface of the Vesta’s crust (e.g., Ono et al., 2016). We found that non-cumulate eucrites contained various silica mineral assemblages though their origins were mostly uncertain. Thus, in this study, we performed a crystallization experiment to see which silica mineral is crystallized from a eucritic magma by rapid cooling comparable to the crystallization of basaltic clasts in non-cumulate eucrites.

2.Sample and Method

We selected the Millbillillie non-cumulate eucrite as a starting material. Millbillillie was grinded into ~10 μm powder and compressed into 125 mg pellets. Then, two pellets were put on Pt wire holders and suspended in a Siliconit vertical electric furnace. They were heated and homogenized at 1300 °C for 48 hours before they were cooled down to 850 °C at 1 °C/hr. Total pressure was 1 atm and oxygen fugacity was controlled at logfO_2=IW-1 using gas mixture of CO_2-H_2. Polished thin sections of the experimental charges were prepared. They were observed by an optical microscope and FE-SEM, and elemental mapping was performed using electron microprobe to locate silica phases. Then, silica polymorphs were identified by EBSD patterns and Raman spectra.

3.Results and Discussion

Lathy plagioclase and pyroxene were observed and silica minerals were present at their grain boundaries in the recovered sample. EBSD patterns and Raman spectra revealed that all silica minerals are cristobalite. These results suggest that cristobalite is the first silica mineral crystallized from eucritic magma by rapid cooling. The occurrence of cristobalite indicates that they are crystallized after crystallization of pyroxene and plagioclase. This experimental result has an implication for interpreting the formation of silica assemblages in non-cumulate eucrites. Aggregates of cristobalite and quartz are present in Yamato-75011. Because a hackle fracture pattern is locally found in cristobalite, it is considered that aggregates formed by partial transformation from cristobalite to quartz, which is consistent with experimental result that cristobalite was the first silica phase. In Pasamonte, there are subhedral cristobalite, quartz, and orthorhombic tridymite. The experimental result suggests that cristobalite first crystallized and then transformed to quartz and orthorhombic tridymite by thermal metamorphism after brecciation. Stannern contains only anhedral quartz. Because of thermal metamorphic level of Stannern (type 4), cristobalite was probably completely transformed to quartz by thermal metamorphism. Therefore, cristobalite is crystallized at first, and then other silica polymorphs are formed by secondary alteration in non-cumulate eucrites.

4.Conclusion

In this study, it is clarified that cristobalite first crystallizes from eucritic magma by rapid cooling (1 °C/hr). This result indicates a possibility that silica polymorphs in non-cumulate eucrites involves different transformation degrees from cristobalite. Such transformation is considered to have been occurred by slower cooling than 1 °C/hr or secondary thermal metamorphism.

Keywords: Silica minerals, Eucrite, Crystallization Experiment, Cristobalite, Quartz, Transformation

Origin of silica minerals in basaltic eucrites

*Rei Kanemaru[1], Akira Yamaguchi[1,2], Hirotsugu Nishido[3]

1. The Graduate University for Advanced Studies, 2. National Institute of Polar Research, 3. Okayama University of Science

Introduction: Eucrites grouped with diogenites and howardites, represent the largest group of differentiated meteorites. Eucrites are considered to have originated from an asteroid 4 Vesta. Eucrites are basalts or gabbros made up the outermost crust of Vesta formed after global melting. After the crust formation, eucrites experienced secondary processes such as shock metamorphism, brecciation, reheating, and metasomatism. Secondary minerals in eucrites provide us with valuable information about post-crystallization history of the eucritic crust. We have been studying the occurrences of silica minerals in basaltic eucrites for better understanding of the secondary processing. In this study, we described the textures of silica minerals in basaltic eucrites with different metamorphic grades [e.g., 1].
Samples and Methods: We studied five Antarctic eucrites (A-881747, EET 90020, Y-790266, Y-792510 and Y 983366) and six non-Antarctic eucrites (NWA 049, NWA 1466, NWA 5356, NWA 7188, Agoult and Juvinas). We examined these eucrites using an electron microprobe analyzer (EPMA JEOL JXA-8200), scanning electron microscope (SEM JEOL JSM 7100) equipped with an EDS (Oxford AZtec Energy) and CL system (Oxford Mono CL2). We used a luminoscope (ELM-3) and a Raman spectroscope (JASCO NRS-2100) to distinguish silica minerals.
Results: We estimated the degrees of thermal metamorphism (petrologic types) [1] for these eucrites. The presence of zoned pyroxene indicates that NWA 049 and Y-790266 are classified into petrologic type 2 and 3, respectively. These eucrites suffered from relatively low degrees of thermal metamorphism. A-881747, Y-792510, Y 983366, NWA 1466, NWA 7188 and Juvinas have low-Ca pyroxene with homogeneous Fe/Mg values indicating that they are classified into petrologic type 4 or 5. These eucrites suffered from moderated degrees of metamorphism. Agoult, EET 90020 and NWA 5356 are classified into petrologic types 5-6. Agoult and EET90020 have granulitic textures, indicative of strong metamorphism. These eucrites may have experienced stronger degrees of metamorphism than did normal type 5-6 eucrites. We classified silica minerals in the eucrites studied here into three groups. (A) Most silica phases in Agoult, EET 90020 and NWA 5356 (type 5-6) occur as tridymite. Tridymite in NWA 5356 contains tiny (< 10 μm) inclusions (anorthite, pyroxene and ilmenite). (B) In NWA 049 (type 2), A-881747, Y-792510, NWA 1466 and Juvinas (type 4 or 5), both tridymite and quartz occur. Tridymite occurs as large lath or rectangular crystals (<500 μm). Tiny grains (<30-50 μm) of quartz (quartz aggregates) occur along rims around and as veins in the tridymite grains. The quartz is in most cases associated with ilmenite and troilite. (C) In Y-790266 (type 3), Y 983366 (type 4) and NWA 7188 (type 4-5), most of the silica phases are quartz. Quartz portions in these eucrites show a fine-grained texture similar texture the (B) group.
Discussion: We could not find any relationship between the petrologic types estimated from pyroxenes and the occurrences of silica minerals except for the highly metamorphosed eucrites. This indicates that the fine-grained quartz formed by secondary processes. The vein-like textures indicate that the quartz aggregate formed after the crystallization of tridymite possibly due to metasomatism. On the other hand, the presence of large grains of tridymite and the absence of quartz is consistent with the fact that Agoult and EET 90020 experienced high-temperature metamorphism (>1000 ˚C).
References: [1] Takeda H. and Graham A.L. (1991) Meteoritics 26, 129-134. [2] Yamaguchi A. et al. (2009) Geochim. Cosmochim. Acta, 73. 7162-7182.

Keywords: eucrites, silica minerals, Cathodoluminescence

Determination of the age of the metal-silicate mixing on the mesosiderite parent body

*Makiko K. Haba[1], Akira Yamaguchi[2], Yi-Jen Lai[3], Jörn-Frederik Wotzlaw[3], Maria Schönbächler[3]

1. Department of Earth and Planetary Sciences, Tokyo Institute of Technology, 2. National Institute of Polar Research, 3. ETH Zurich

Mesosiderites are polymict breccias composed of roughly equal amounts of silicates, which are similar to HED meteorites, and Fe-Ni metal. This meteorite group has been thought to have formed by mixing of crustal and core materials without including much of the mantle. Although several scenarios have been proposed for the metal-silicate mixing, the origin of Fe-Ni metal that was molten at that time and the mechanism of the mixing event are still open questions. Therefore, a well-constrained age of the metal-silicate mixing is important information to improve our understanding of the formation process of mesosiderites. Although the Sm–Nd and Mn–Cr ages of mesosiderites have revealed that the metal-silicate mixing occurred 20–150 Ma after the solar system formation (Stewart et al., 1994; Wadhwa et al., 2003), the age still has a large range more than 100 million years. In order to determine a more precise age of the metal-silicate mixing event, it is necessary to analyze the minerals which had formed during the mixing event. Also, it is necessary that the sample has remained closed systems for chronometers throughout the later impact events. In this study, we present the ^{92}Nb-^{92}Zr and U-Pb ages of mesosideritic rutiles and zircons in consideration of the formation mechanisms of the minerals. The goal of this study is to determine the age of the metal-silicate mixing event that formed mesosiderites.

Four mesosiderites having different metamorphic grades, Vaca Muerta (1A), NWA 1242 (2A), A 882023 (2/3A), and Estherville (3/4A), were used in this study. Rutiles and zircons were separated from residual samples after dissolving the metal parts and silicate parts with concentrated acids. Subsequently, rutile grains were dissolved in HNO_3-HF using Parr® bombs. The Nb/Zr ratio and Zr isotope measurements were performed using a quadrupole ICPMS and a Neptune Plus MC-ICPMS, respectively, at ETH Zurich. Four individual zircons (70–200 μm in diameter) were spiked with 3–5 mg of EARTHTIME ^{202}Pb-^{205}Pb-^{233}U-^{235}U tracer solution and dissolved in concentrated HF using Parr® bombs. U and Pb were separated using a HCl-based column chemistry and measured using a TRITON Plus TIMS at ETH Zurich.

The rutiles from each sample yielded ^{93}Nb/^{90}Zr ratios of 12.7 ±0.8 in Vaca Muerta, 9.9 ±0.4 in NWA 1242, 1.61 ±0.12 in A 882023, and 1.26 ±0.08 in Estherville. The ^{93}Nb/^{90}Zr ratios decrease with increasing metamorphic grades of our samples from Vaca Muerta (1A) to NWA 1242 (2A), A 882023 (2/3A), and Estherville (3/4A). Since the metamorphic grades of mesosiderites were established during the metal-silicate mixing event (e.g., Delaney et al., 1981), the rutiles likely formed during this event. The Nb-Zr data from rutiles are plotted on a single isochron line (Fig. 1), which indicates that the ^{92}Nb-^{92}Zr decay system of mesosideritic rutiles has not been disturbed by later impacts after they formed during the metal-silicate mixing event. Using the initial ^{92}Nb/^{93}Nb ratio of rutiles ((7.5 ±0.7) ×10^{-6}) and the solar system initial ^{92}Nb/^{93}Nb ratio from Iizuka et al. (2016), the ^{92}Nb-^{92}Zr age of rutiles was calculated to be 44 ±16 Myr after CAI. This age corresponds to the absolute age of 4524 Ma.

According to Haba et al. (2015), mesosiderites have two kinds of zircons: (I) relict zircons that crystallized before the mixing event, and (II) secondary zircons that formed through the mixing event. Typical secondary zircons show quite low U (~0.3 ppm) and Th (~0.04 ppm) contents because they formed after the incorporation of U, Th, and REE into abundant phosphate minerals. All zircon grains measured in this study have very low U contents, which indicate that they are secondary zircons, and yielded a weighted mean ^{207}Pb-^{206}Pb age of 4528.4 ±1.4 Ma (2σ). This age is in good agreement with the ^{92}Nb-^{92}Zr age of rutiles. Therefore, the metal-silicate mixing event that formed mesosiderites is considered to have

occurred at 4528.4 ±1.4 Ma.

Keywords: mesosiderites, metal-silicate mixing event, radiometric dating, zircon, rutile

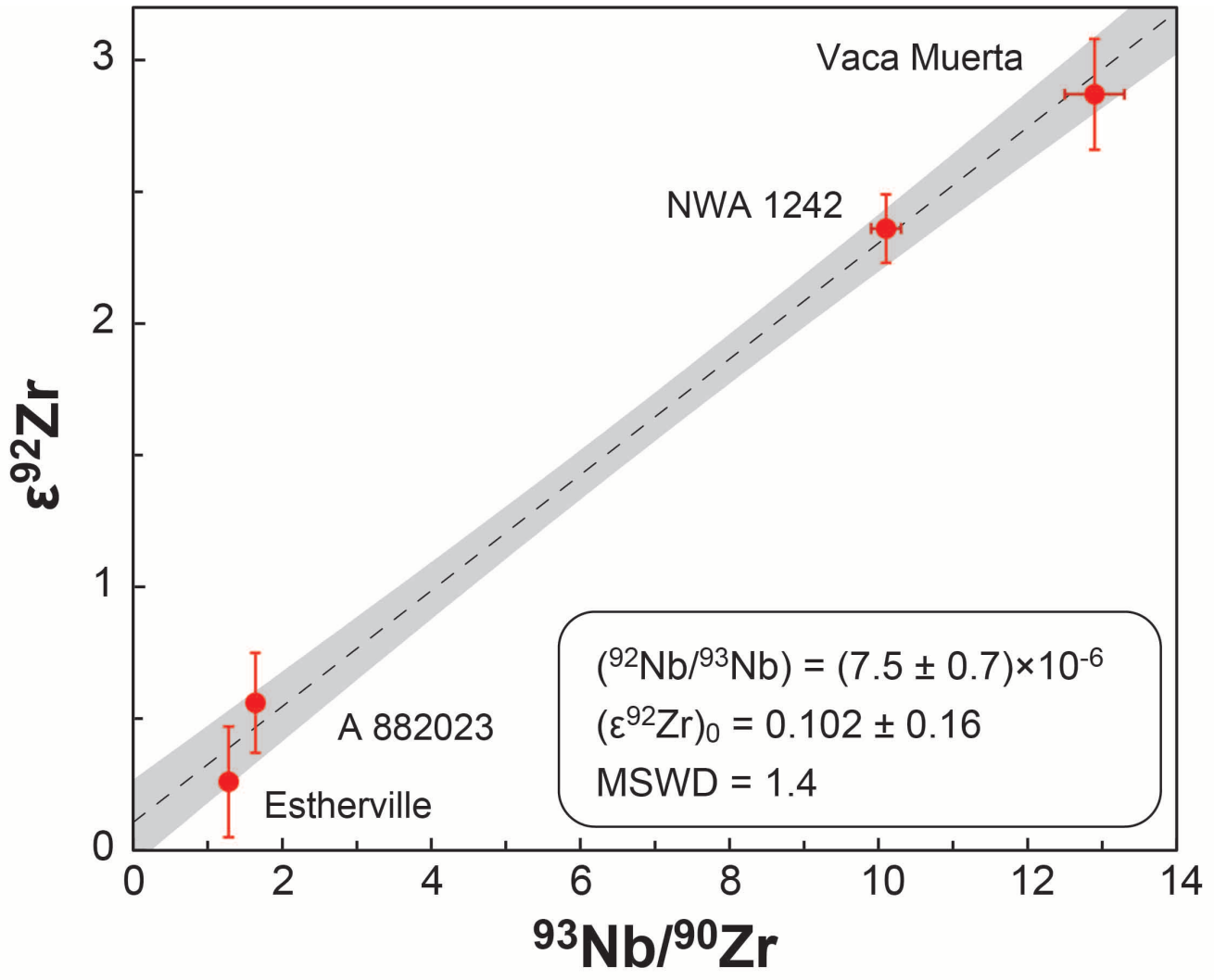

Fig. 1. Nb-Zr isochron diagram for mesosideritic rutiles. The isochron regression and error envelope (95% probability) are shown as a dotted line and gray area, respectively. The data-point errors are 2 σ.

Hf-W chronology of the pallasite Brenham

*Yoshitaka Homma[1], Tsuyoshi Iizuka[1]

1. Department of Earth and Planetary Science, The University of Tokyo

Pallasites are stony-iron meteorites consisting mainly of rounded olivine and metal. The formation process of the pallasite meteorites have been investigated from the petrological and chemical data, but it is still enigmatic. Two major hypotheses are considered: (i) fractional crystallization of olivine at core-mantle boundary on their parent bodies and (ii) metal-silicate mixing generated by a catastrophic impact. Determining the precise age of the pallasites and, more preferably, their constituent phases, are key to constraining the formation process and the nature of the parent bodies. In this study, Hf-W isotopic analyses have been performed on metal, olivine, and non-magnetic fractions of Brenham, a main group (MG) pallasite. Taking into account the effects of neutron capture and nucleosynthetic anomaly, the ε^{182}W value of the Brenham metal fraction is determined as -3.43 +0.23/-0.30. The tungsten isotopic value of Brenham metal corresponds to a model age of -0.22 +2.94/-3.34 Myr after the CAI formation. The result indicates that the differentiation on the MG pallasite parent body had occurred within the first 2.7 Myr of the solar system history. We further reveal that the olivine and non-magnetic fractions yielded substantially higher ε^{182}W value than the metal fraction. Extrapolating an internal isochron using the metal and olivine fraction data yields an age older than the CAIs. This unrealistically old age would be attributed to the apparent elevated ε^{182}W values of the olivine fractions due to neutron capture. Such neutron capture effect on the ε^{182}W values can be potentially corrected by analyzing Hf stable isotopes in the fractions.

Keywords: stony-iron meteorite, Hf-W chronology, core-mantle differentiation

Determination of highly siderophile elements and osmium isotope compositions in metal phases from CR chondrites using micro sampling technique

*Nao Nakanishi[1], Tetsuya Yokoyama[1], Satoki Okabayashi[1], Kiwamu Shimazaki[1], Tomohiro Usui[1], Hikaru Iwamori[1,2]

1. Tokyo Institute of Technology, 2. Agency for Marine-Earth Science and Technology

Metal plays a key role in physicochemical processes that fractionate siderophile elements from lithophile elements in the early solar system, generating variable chemical reservoirs before the onset of planetesimal formation. Highly siderophile elements (HSEs: Re, Os, Ir, Ru, Pt and Pd) have great affinity for Fe-Ni metals relative to silicates. HSEs are refractory and exist as gas only at high temperatures. Therefore, geochemical investigation on HSEs in metal phases for a variety of meteorites can provide an important clue for understanding high temperature processes in the solar nebula. In particular, the ^{187}Re-^{187}Os isotope system gives chronological information regarding the fractionation of HSEs.
CR chondrites contain 40–60 vol. % of chondrules with 5–8 vol. % of metal grains and have unique characteristics for the coexistence of metal phases with chondrules [1, 2]. Therefore, CR chondrites are suitable for understanding the genetic linkage between metals and chondrules. Metal grains are found in three different locations of CR chondrites; chondrule interior (“interior grain”), chondrule surficial shells (“margin grain”), and the matrix (“isolated grain”). Previous studies on CR metals [2, 3] suggested that CR metals could have formed via melting and recondensation of surrounding vapor, although the details for the origin of CR metals remains unclear.
In this study, we tried to established a formation model for the series of three types of CR metals based on their HSE abundances and Os isotope compositions. We prepared thick sections of three CR chondrites: NWA 801, NWA 7184, and Dhofar 1432. The petrography and the mineral compositions of these sections were examined with SEM-EDX (Hitachi 3400; Bruker Xflash 5010). We analyzed the abundances of HSEs, major (Fe and Ni), and minor (P, S, Cr, and Co) elements for multi-spots of these grains using fs-LA-ICP-MS (IFRIT, Cyber Laser) and EPMA (JEOL-JXA-8530F), respectively. In addition, we determined Os isotope compositions for two isolated grains in NWA 801. The details for Os isotope analysis using a micro milling system and N-TIMS (TRITON plus, Thermo Fisher Scientific) are described in [4].
The Pd/Ir ratios in all types of CR metal grains decreased rapidly with the increase of Ir concentration. Equilibrium condensation of metals from a gaseous reservoir does not account for the large variation of Pd/Ir. From the HSE abundances in metal grains obtained, we calculated the partition coefficients (*D*) of HSEs between solid and liquid metals. We found that the order of *D* values determined for individual HSEs were consistent with those calculated from the experimental partitioning data [5]. Next, we estimated the initial composition of metal phases that fits the observed data points using the fractional crystallization model. The Ir-normalized initial HSE abundances are all chondritic excluding the Pd/Ir ratio. We speculate that Pd could have been lost during chondrule formation process before metal crystallization, because Pd is relatively volatile among the HSEs. From these evidences, we conclude that CR metals have most likely formed via fractional crystallization.
We found that two isolated metals analyzed have ^{187}Os/^{188}Os ratios (0.1258, 0.1261) close to that of bulk CI (0.1263–0.1265) and CR (0.1253–0.1271) chondrites [6]. Such consistent Os isotope ratios suggest that isolated grains in CR chondrites have formed from a CI-like precursor with preserving the original CI-like ^{187}Os/^{188}Os ratio without substantial Re-Os fractionation. This scenario is supported by the chondritic HSE (excluding Pd) initial abundances in CR metals estimated by the fractional crystallization

model.

References: [1] Lee et al. (1992) GCA, 56, 2521–2533. [2] Jacquet et al. (2013) MAPS, 48, 1981–1999. [3] Connolly et al. (2001) GCA, 65, 4567–4588. [4] Nakanishi et al. (2013) LPSC, abstract #2407. [5] Chabot and Jones (2003) MAPS, 38, 1425–1436. [6] Walker et al. (2002) GCA, 66, 4187–4201.

Keywords: chondrite, metal phase, Osmium isotopes, CR chondrtie

Mineralogical and petrological study of plagioclase-bearing lodranite, Yamato 981988.

*Masahiro YASUTAKE[1], Akira Yamaguchi[1,2]

1. Dept. of Polar Science, SOKENDAI, 2. National Institute of Polar Research

Introduction Primitive achondrites are meteorites that have both chondritic and achondritic features. Acapulcoite-lodranite clan is the second largest clan of primitive achondrites [1]. Acapulcoites and lodranites are primarily distinguished based on their grain sizes. Acapulcoites have finer-grained textures (~0.2 mm) whereas lodranites have coarser-grained textures (~0.5-0.7 mm) [2, 3]. Acapulcoites have chondritic modal abundances and bulk chemical compositions. Most lodranites have modal abundances depleted in plagioclase and/or troilite and fractionated bulk chemical compositions. Several transitional acapulcoite-lodranite meteorites have been found. The transitional group has larger grain sizes than acapulcoites, whereas they have modal abundances rich in plagioclase and bulk chemical compositions relatively similar to acapulcoites rather than lodranites [4, 5, 6]. The transitional group provides us with the further clues on the igneous and metamorphic processes on the parent body.
Samples and methods We investigated one polished thin section (PTS) of Y 981988. The PTS was observed by an optical microscope and a FE-SEM (JEOL JSM 7100F). Mineral compositions were obtained by using of an EPMA (JEOL JXA8200). The lattice preferred orientations (LPO) were measured by using of an EBSD detector (Oxford instruments AZtec HKL) mounted on the FE-SEM.
Results Y 981988 shows a coarse-grained texture (~0.7 mm) mainly consisting of olivine (43 vol.%) (Fo_{93}), orthopyroxene (34 vol.%) ($Wo_{3.0}En_{88}$) plagioclase (10 vol.%) ($Or_{2.5\text{-}4.8}Ab_{78\text{-}84}$), and Fe,Ni-metal (6 vol.%). Plagioclase occurs interstitially. Some plagioclases partly or entirely enclose olivine and orthopyroxene grains. The lattice preferred orientations of plagioclase crystals are the same in wide areas up to ~6mm width. The PTS contains a large augite crystal (~7 mm) ($Wo_{43\text{-}46}En_{50\text{-}53}$) that poikilitically encloses olivine and orthopyroxene chadacrysts. Minor mineral includes phosphate, schreibersite, troilite and chromite (molar Cr/(Cr+Al)x100 = 14-16, molar Fe/(Fe+Mg)x100 = 51-57). The pyroxene equilibration temperatures [7] are estimated to be ~1120˚C from orthopyroxene and ~1090˚C from augite. These temperatures are similar to those of other lodranites [2].
Discussion The mineral compositions are within the range of acapulcoite-lodranite meteorites. The coarse-grained texture favors that Y 981988 is a lodranite. However, modal abundance rich in plagioclase is similar to acapulcoites rather than lodranites.
McCoy et al. [3] found that plagioclase modal abundances among lodranites are correlated with Fa content of olivine, except for EET 84302. They argued that relatively large abundances of plagioclase were caused by low degree of silicate partial melting. They indicated that mafic silicate compositions or low peak temperatures caused low degree of partial melting. The modal abundance of plagioclase of Y 981988 is not correlated with olivine composition.
These observations indicate that Y 983119 suffered silicate partial melting over the solidus temperature, but probably did not experience removal of silicate melt. We suggest that Y 981988 is a transitional acapulcoite-lodranite meteorite.
Reference [1] Weisberg et al., (2006), *Meteorites and the early solar system II,* 19-52. [2] McCoy et al., (1996), *GCA*, 60, 2681-2708. [3] McCoy et al., (1997), *GCA*, 61, 3, 623-627. [4] Yugami et al., 1998, *Antarct. Meteorit. Res.*, 11, 49-70. [5] Floss, (2000), *Meteortit. Planet. Sci.*, 35, 1073-1085. [6] Patzer et al., (2004), *Meteorit. Planet. Sci.*, 39, 1, 61-85. [7] Lindsley, (1983), *Ame. Mineral.,* 68, 477-493.

Keywords: Meteorite, Primitive achondrite, Acapulcoite-lodranite meteorite

Hydrogen diffusion experiment of fluorapatite under water vapor conditions

*Yoshinori Higashi[1], Shoichi Itoh[1], Ken Watanabe[2,3], Isao Sakaguchi[3]

1. Graduate School of Science, Kyoto University, 2. Interdisciplinary Graduate School of Engneering Sciences, Kyushu University, 3. National Institute for Materials Sience

Apatite [$Ca_5(PO_4)_3$(F, Cl, OH)] contains highly volatile elements such as F, Cl, and OH in the anion sites, making it a useful recorder of volatile components and water in fluids and magmas in the Earth and extraterrestrial bodies (e.g., [1]). Many studies in the past decade have sought to explore the origin and evolution of water in planetary bodies based on the water contents and hydrogen isotopic compositions of apatite (e.g., [2][3]). However, without an understanding of hydrogen diffusivity in apatite, it is difficult to estimate whether original hydrogen isotopic compositions from crystallization are preserved, or the subsequently modified by reactions with water after crystallization. Therefore, it is necessary to understand the hydrogen diffusivity in apatite during water–rock interactions. Recently, hydrogen diffusion coefficient of fluorapatite parallel to the *c*-axis was reported [4]. Here we report hydrogen diffusivity of the anisotropy and the water content dependence of hydrogen diffusion to compare with that of *c*-axis [4].

In order to investigate the water content dependence of hydrogen diffusion, natural fluorapatite crystals that have different water content (from Durango, ~500 ppm H_2O [2] and Morocco, ~4000 ppm H_2O [5]) were used for diffusion experiment. To investigate the anisotropy of hydrogen diffusion in apatite, Durango apatite crystals were cut in two directions for the crystallographic *c*-axis (parallel or normal to the *c*-axis). Hydrogen diffusion experiments using these natural fluorapatites were carried out under a saturated D_2O/O_2 vapor flow at temperatures of 500–700 ˚C. Diffusion depth profiles for ^1H and ^2D were measured using secondary ion mass spectrometry (CAMECA ims 4f-E7 SIMS), indicating that ^2D diffusion occurred by an exchange reaction between the original ^1H and ^2D during annealing. Hydrogen diffusion coefficients were obtained by the fitting of diffusion profiles of ^2D using Fick’ s second law; they followed an Arrhenius-type relationship.

Hydrogen diffusion in Durango apatite normal to the *c*-axis is approximately five times faster than that of along to the *c*-axis. Variation in water content of apatite would not lead to large changes in the hydrogen diffusivity. The similarities of the activation energy for hydrogen diffusion in apatite and hydrous minerals suggest that hydrogen in apatite lattice is transported via the Grotthuss mechanism like other hydrous minerals [6]. Hydrogen diffusion coefficients in apatite are several orders of magnitude greater than those of other elements. This study indicates that the hydrogen isotopic compositions of apatite are readily affected by the presence of water vapor through the H–D exchange reaction without changing the total water content in the crystal. Hydrogen diffusion of apatite crystals would play an important role to determine the hydrogen isotopic compositions of apatite in extraterrestrial bodies.

References

[1] Harlov (2015) *Elements*, **11**, 171–176. [2] Greenwood et al. (2011) *Nature Geosci.*, **4**, 79–82. [3] Usui et al. (2015) *Earth Planet. Sci. Lett.*, **410**, 140–151. [4] Higashi et al. (2017) *Geochem. J.* **51**, 115–122. [5] McCubbin et al. (2015) *Am. Mineral.*, **100**, 1668–1707. [6] Marion et al. (2001) *Am. Mineral.*, **86,** 1166–1169.

Keywords: Hydrogen, Apatite, Diffusion, SIMS

Water Content Analyses on Apatite Grains in H Chondrites by NanoSIMS : Application of Indium Mounting Method

*Satoki Onda[1], Mizuho Koike[1], Naoto Takahata[1], Yuji Sano[1], Kenji Shimizu[2]

1. Atmosphere and Ocean Research Institute, the University of Tokyo, 2. Kochi Core Center, Japan Agency for Marine-Earth Science and Technology

Although ordinary chondrites have been thought as anhydrous, existence of halite [NaCl] is reported in some fallen H chondrites [1][2], which implies that parent bodies of H chondrites were involved with water. The origin of water in the parent bodies of ordinary chondrites is still unknown. It is proposed that the water might be taken into parent bodies at the time of accretion, or added when icy objects, like comets, had collisions with the parent bodies [1]. Revealing the origin of water in ordinary chondrite parent bodies is significant for understanding the behavior of water in the early solar system. In this study, we focused on H type chondrites.

Apatite [Ca5(PO4)3(F,Cl,OH)] is a phosphate mineral which contains OH^- , F^- or Cl^-. Apatite grains are commonly found on meteorites including H chondrites, and they retain information about volatile elements such as water or halogen [3]. Moreover, it is proposed that formation process of some apatite grains in H chondrites is related to halite [2]. Therefore, apatite grains are expected to be important for understanding the behavior of water in the parent bodies. However, measuring water content of apatite grains in H chondrites had a technical difficulty due to their low water content (~100-1000 ppm [2]). Secondary Ion Mass Spectrometer (SIMS) is an effective method to know in-situ water content of samples with low water content. For SIMS method, meteorite samples are generally mounted in epoxy resins. As epoxy resins fill voids in samples well, the method is suitable for fragile samples including meteorites. However, resins have large influence on water analyses because the resins, which is organic materials, get into the voids. For water content or hydrogen isotopic ratio measurements of meteorite samples, the epoxy-resin method is not suitable due to the contamination from resins because meteorite samples generally have a lot of voids.

Therefore, we focused on another method; mounting solid samples in metallic indium [4][5][6]. Indium has a low melting temperature (~156˚C), and it can be easily cut or formed into preferable shapes. Indium-mounted samples have less influence than samples in epoxy resins, because indium contains smaller amount of water and get into voids less than resins, though the samples in indium is not fixed as those in epoxy resins. Therefore, it is expected that we can conduct water content or hydrogen isotopic ratio analyses on the samples with lower water content (H2O~100-1000ppm) by SIMS using the indium-mounting method. In fact, the indium-mounting method is confirmed to be effective for reducing hydrogen background counts of SIMS analyses; De Hoog et al. (2014) [4] report that H^+ background counts were 165-180 cps for samples mounted in epoxy resins, and 18-21 cps for indium-mounted samples, in their measurements on zircon from Mid-Atlantic Ridge by Cameca 4f.

We conducted water content and hydrogen isotopic ratio analyses on apatite standards and terrestrial olivine (from San Carlos, Arizona) mounted in epoxy resins and indium by NanoSIMS 50 at Atmosphere and Ocean Research Institute, the University of Tokyo, to compare with each other. Moreover, we conducted water content analyses on apatite grains in H chondrites mounted in indium and discussed the origin of water in parent bodies of H chondrites.

References:

[1] Zolensky et al. (1999) Science, **285**, 1377-1379.

[2] Jones, McCubbin & Guan (2016) Amer. Min., **101**, 2452-2467.
[3] McCubbin & Jones (2015) Elements, **11**, 183-188.
[4] De Hoog et al. (2014) GCA, **141**, 472-486.
[5] Usui et al. (2012) EPSL, **357-358**, 119-129.
[6] Shimizu et al. (2017) Geochem. J. (accepted)

Keywords: apatite, H chondrite, water content, NanoSIMS, indium mounting

High precision Sr isotope measurements for bulk chondrites with complete sample digestion

*Ryota Fukai[1], Tetsuya Yokoyama[1], Wataru Okui[1], Sho Hasegawa[1]

1. Department of Earth and Planetary Sciences, Tokyo Institute of Technology

Nucleosynthetic isotope anomalies have been discovered in bulk chondrites and differentiated meteorites for various refractory heavy elements (e.g., Cr, Ru [1, 2]). In the most cases, the extent of isotope anomalies is variable across different types of meteorites. These results point to the existence of planetary-scale isotope heterogeneities, which are most likely due to the incomplete mixing of dust grains and/or selective destruction of presolar grains during thermal processing in the early solar nebula. However, the processes that have led to the observed isotope heterogeneity are not fully understood. High precision stable Sr isotope analyses on bulk meteorites have been conducted in some previous studies ([3–5]). These studies found isotopic variations of $^{84}Sr/^{86}Sr$ ratios across three types of chondrites (enstatite, ordinary, and carbonaceous chondrites). However, the extent of Sr isotope heterogeneities across entire classes of chondrites remains unclear due to the limited number of Sr isotope data with sufficiently high precision. In addition, not all studies have performed complete digestion of samples that contained acid resistant presolar grains.

In this study, we revisited high precision Sr isotope analysis of chondrites coupled with a robust sample digestion technique that confirmed complete dissolution of presolar grains. We also improved the analytical reproducibilities of Sr isotope measurement from previous studies by adopting the dynamic-multicollection method with TIMS.

The reproducibilities for NIST 987 standard obtained in a single analytical campaign were 16 ppm for $^{84}Sr/^{86}Sr$ ratio (n = 7, 2SD), which are two times superior to those in previous studies [3–5]. We investigated four enstatite chondrites (EH and EL), seven ordinary chondrites (H, L, and LL), and four types of carbonaceous chondrites (CI, CM, CO, and CV). Three types of ordinary chondrites possess generally uniform $\mu^{84}Sr$ values* (= −12 ±29 ppm; 2SD). By contrast, enstatite and carbonaceous chondrites possess variable Sr isotopic compositions depending on each subgroup. For instance, EL chondrites show the lowest $\mu^{84}Sr$ values (= −30 ±26 ppm) among all types of chondrites, while EH chondrites show $\mu^{84}Sr$ values indistinguishable from ordinary chondrites (= −12 ppm ±36 ppm). On the other hand, a CI chondrite (Y-980115) shows $\mu^{84}Sr$ values (= 14 ±14 ppm) that is resolved from those of CV chondrite (Allende) showing the highest $\mu^{84}Sr$ values (= 36 ±21 ppm) among all types of chondrites. The observed global trend for the $\mu^{84}Sr$ value that range from −30 ppm for EL chondrites to 36 ppm for CV chondrites is consistent with the results of other heavy refractory elements (e.g., Mo [6], Ru [2], Nd [7]), which have been induced most likely by the selective destruction for presolar grains via nebular thermal processing. Furthermore, the existence of the local trend observed in carbonaceous chondrites would reflect the additional processes that may have occurred in the outer Solar System before the accretion to each parent body for carbonaceous chondrites.

* Parts par 10^6 relative deviation from the standard, NIST 987

[1] Trinquier, A. et al. (2007) *ApJ,* **655**, 1179. [2] Fischer-Gödde, M. and Kleine, T. (2017) *Nature*, **541**, 525. [3] Moynier, F. et al. (2012) *ApJ*, **758**, 45. [4] Paton, C. et al. (2013) *ApJL*, **763**, 40. [5] Yokoyama, T. et al. (2015) *EPSL*, **416**, 46. [6] Burkhardt, C. et al. (2011) *EPSL*, **312**, 390. [7] Gannoun, A. et al. (2011) *PNAS,* **108**, 7693.

Keywords: Isotope anomalies, chondrites, high precision isotope analysis

Origin of Mo isotope dichotomy between carbonaceous chondrites and non-carbonaceous meteorites

*Yuichiro Nagai[1], Tetsuya Yokoyama[2], Takafumi Hirata[1]

1. Geochemical Research Center, Graduate School of Science, The University of Tokyo, 2. Department of Earth and Planetary Science, School of Science, Tokyo Institute of Technology

The existence of nucleosynthetic isotope anomalies for refractory heavy elements in bulk meteorites evidently points to the heterogeneous distribution of dust grains with distinct isotopic compositions in the early solar nebula. Molybdenum is a promising element for the study of nucleosynthetic isotope anomalies in meteorites; previous studies found that bulk meteorites and their constituents including CAIs, chondrules, and presolar materials had nucleosynthetic isotope variations for Mo [1-6]. Recently, Warren [7] discovered isotopic dichotomy for O, Ti, and Cr between carbonaceous chondrites (CCs) and non-carbonaceous meteorites (NCs: ordinary, enstatite, and rumuruti chondrites, differentiated meteorites). Budde et al. [2] suggested that Mo isotopic compositions for CCs and their components could be discriminated from those of NCs. However, highly precise Mo isotopic data for NCs are limited so far because of analytical difficulties. In this study, we provide high precision Mo isotope data for NCs measured with N-TIMS to better understand the origin of source materials for NCs that represent the materials existed in the inner part of the early Solar System.

Molybdenum isotope analyses for nineteen NC samples from ten meteorite groups (ordinary chondrites: H, LL; rumuruti chondrites; irons: IIAB, IIE, IIIAB, IVA, IVB, ungrouped) have been made in this study. The meteorite samples were dissolved with HF–HNO_3 and HCl–HNO_3. Molybdenum was purified by employing two-stage chemical separation technique [8]. Molybdenum isotope analysis was performed with N-TIMS using TRITON *plus* (Thermo Fischer Scientific Inc., Bremen) installed at Tokyo Institute of Technology [9].

The extent of Mo isotope anomalies for NCs is clearly discriminated from that of CCs. Most importantly, the data points for NCs defined a positive linear correlation on the μ^{94}Mo–μ^{95}Mo diagram passing through the origin (i.e., Earth's composition), whereas those for CCs deviate from the Earth–NCs correlation line. An exception is that IVB irons and ungrouped irons (Chinga) have Mo isotopic compositions similar to CCs, presumably indicating that the parent bodies for these irons have formed under the physical condition (e.g., fO_2) similar to those of CC parent bodies [10-11]. Our observation suggests the existence of contributor which produced Mo isootpic difference between NCs and CCs. A possible carrier phase that involved in this difference is the type X presolar SiC enriched in ^{95}Mo and ^{97}Mo [6], although a dominant contributor of Mo isotope anomalies are considered to be the mainstream SiC [3].

Based on the data presented here, we propose that the observed Mo isotopic dichotomy has been formed across the formation region of meteorite parent bodies by the time when parent bodies of irons have accreted. The accretion of iron parent bodies for NCs (IIAB, IIAB, and IVA) and for presumed CCs (IVB) occurred within 0.3 Myr after CAI formation in the basis of the Hf–W system along with the S contents in irons [12]. The early formation of the two reservoirs regarding Mo isotope anomalies could be associated with the dramatic migration of giant planets that ultimately disturbed the composition of asteroid belt [13]. Therefore, determination of the timing of giant planet formation is crucial to decode the origin of Mo isotope dichotomy.

* $\mu^{i}\mathrm{Mo} = [(^{i}\mathrm{Mo}^{96}\mathrm{Mo})_{\mathrm{sample}}(^{i}\mathrm{Mo}^{96}\mathrm{Mo})_{\mathrm{std}} -1] \times 10^{6}$

reference: [1] Burkhardt et al. (2011) *EPSL*, **312**, 390. [2] Budde et al. (2016) *EPSL*, **454**, 293. [3] Nicolussi et al. (1998a) *GCA*, **62**, 1093. [4] Nicolussi et al. (1998b) *ApJ*, **504**, 492. [5] Savina et al. (2007) *LPSC*, **38**, #2231. [6] Pellin et al. (2006) *LPSC*, **37**, #2041. [7] Warren (2011) *EPSL*, **311**, 93. [8] Nagai and Yokoyama (2014) *Anal. Chem.*, **86**, 4856. [9] Nagai and Yokoyama (2016) *JAAS*, **31**, 948. [10] Campbell and Humayun (2005) *GCA*, **69**, 4733. [11] Walker et al. (2008) *GCA*, **72**, 2198. [12] Kruijer et al. (2014) *Science*, **344**, 1150. [13] Walsh et al. (2011) *Nature*, **475**, 206.

Keywords: meteorite, early solar system, molybdenum, isotope anomaly

Zn stable isotope contribution to constraint ureilite formation process

*Genevieve Claire Hublet[1], Vinciane Debaille[2], Luc S Doucet[2], Richard C Greenwood[3], Akira Yamaguchi[1], Nadine Mattielli[2]

1. National Institute of Polar Research, 2. Université Libre de Bruxelles, 3. The Open University

Ureilites are ultramafic achondrites. They are usually considered to be derived from a single parent body (UPB) now-disrupted. There are mainly composed of olivine and pigeonite. This is already demonstrated that ureilites are mantle restites. But, this hypothesis is not consistent to explained preservation of the primitive characteristics such as the O heterogeneity in ureilites [1] and confirmed by the new $\Delta^{17}O$ data in our samples. In this study, we report new Zn stable isotopic composition and also ^{26}Al-^{26}Mg systematic for seven monomict ureilites Yamato (Y) 790981, Y 791538, Y 981750, Y 981810, Asuka (A) 881931, Allan Hills (ALH) 81101 and ALH 84136 to constraint the ureilite formation by smelting process.
Zn isotope analysis of our seven samples yielded non-chondritic and heterogeneous composition in δ^{66}Zn signatures ranging +0.61 ±0.01‰ to +2.68 ±0.11‰. This heterogeneity in Zn can reflected the isotopic signature of the precursor(s). In opposition, Zn is a moderately volatile element, and alternative explanation already mentioned by previous studies suggested this heavy isotope enrichment may reflect volatilization process following major impact [2]. This explanation is generally supported by the correlation between the δ^{66}Zn and the Zn abundance in ureilites. However, this hypothesis is not well supported by the shock degrees. In our study, we evaluated the possibility that δ^{66}Zn signature could be produced by smelting process during ureilites genesis like already suggested by [3-4]. To evaluate the effects of such a volatilization process during smelting, we modeled the Zn isotope fractionation in ureilites on the basis of the Rayleigh distillation equation, according to [5] when Zn isotope fractionation was explored during the smelting process in the metallurgic industry. In this model, we made the assumption that UPB precursor had an initial composition in Zn content and δ^{66}Zn signature similar to a CI type chondrite. The smelting degrees of our samples were evaluated based on their Zn content. Based on this assumption, we show that the observed δ^{66}Zn variability in our ureilites match the data obtained using the smelting process model.
On the other hand, smelting process can occur only if the UPB precursor starts to melt. During this step, the ureilite witch is the residues should be depleted in incompatible elements like suggested by the REE pattern in ureilites [6]. Based on the new REE data [6] and our data, we evidenced correlation between $(Dy/Lu)_n$ ratios and the degrees of smelting modeled. This observation suggests that smelting degrees increased with the degrees of melting (F).
Finally, based on ^{26}Al-^{26}Mg isotopic system, no isochron has been obtained with the $\delta^{26}Mg^*$ and $^{27}Al/^{24}$Mg data analyzed in our samples. If all these samples crystallized at the same time, the $\delta^{26}Mg^*$ data suggest our samples could come from different parent bodies. However, our data set could also reflect different crystallization ages from a single parent body. Considering the smelting process for ureilites formation, this hypothesis could be considered since smelting was a local process. Assuming all the ureilites originated from a single parent body with a chondritic composition, a model age can be determined. This model age reflects the time when the ureilite common source differentiated from a chondritic reservoir. This differentiation can be modeled at 1.09 ±0.75 Ma after the CAI formation.
[1] Clayton R. & Mayeda T. (1988) GCA, 52, 1313-1318. [2] Moynier F. et al. (2010) Chem. Geol., 276, 374–379. [3] Singletary S. & Grove T. (2003) Meteorit. Planet. Sci., 38, 95-108. [4] Goodrich C.A. et al. (2007) GCA, 71, 2876-2895. [5] Mattielli N. et al. (2009) Atmos. Environ., 43, 1265-1272. [6] Barrat J.-A. et al. (2016), GCA, 194, 163-178

High precision Mg isotopic measurement of chondrules from ordinary chondrite meteorite using MC-ICPMS

Akinobu Hayakawa[1], Kohei Fukuda[1], Tsuyoshi Iizuka[1], *Hajime Hiyagon[1]

1. Graduate School of Science, The University of Tokyo

Aluminum-26, a short lived-nuclide with a half life of 0.73 My, has been widely used for discussing relative ages of planetary materials. Based on precise measurements of Al-Mg isotopes in Calucium-aluminum-rich inclusions (CAIs, the oldest solids of the solar system), the initial $^{26}Al/^{27}Al$ ratio at the birth of the solar system has been determined to be 5.25 x10^{-5} [1,2]. It has also been argued that chondrules, a major component of chondritic meteorites, formed at 150 to 400 My after CAI formation [3]. Recently, however, precise U-Pb dating suggested that some chondrules might have ages as old as CAIs [4]. Furthermore, recent Al-Mg isotopic measurements of angrites (achondrites) of known U-Pb ages gave a much lower value of 1.33 x10^{-5} for the initial $^{26}Al/^{27}Al$ ratio of the solar system [5]. These conflicting data suggest a possibility of heterogeneous distribution of ^{26}Al in the early solar system. Distribution of ^{26}Al in the early solar system has crucial importance chronologically (i.e., justification of the Al-Mg chronometer) and also in view of an important heat source for understanding evolution of planets (e.g., their differentiation processes). In order to discuss its distribution, precise measurements of Al-Mg isotopes for various components (CAIs, chondrules, etc.) in various types of chondrites. Among them, there have been very few analyses for chondrules, and they are limited to those in carbonaceous chondrites [e.g., 6,7]. In order to better understand spacial distribution of ^{26}Al in the early solar system, we have developed a high precision Mg isotope analysis technique using MC-ICPMS. Using this technique, we have analyzed three CV CAIs to examine if our analysis give a canonical $^{26}Al/^{27}Al$ ratio consistent with previous works. We have also applied the technique to chondrules in an ordinary (LL) chondrite and compared the results with those of carbonaceous chondrite (CC) chondrules and discussed distribution of ^{26}Al in the early solar system.

The analyzed samples were two CAIs from NWA 3118 (CV3), a CAI from Allende (CV3) and 6 chondrules from NWA 7936 (LL 3.15). We have prepared a Mg isotope standard DSM-3 (pure solution of terrestrial Mg [8]), and all the Mg isotope results (excess ^{26}Mg) were expressed as $\mu^{26}Mg^*$ (i.e., ppm deviation from the result of DSM-3). The results for two terrestrial standards, BCR-2 and JB-2, gave $\mu^{26}Mg^*$ values of -5.9 ±11.2 and 2.3 ±20.0, respectively, i.e., good precision and accuracy comparable to those by other laboratories [e.g., [9]]. If we apply a single isochron for the data of three CAIs, we obtain $(^{26}Al/^{27}Al)_o$ = (5.08 ±0.84) x10^{-5} from the slope and $\mu^{26}Mg^*$ = -25 ±103 ppm from the y-intercept, which are consistent with previous studies [1,2].

Five out of 6 LL chondrules show Al/Mg ratios (0.091-1.04), similar to the solar composition (~0.10). If we assume homogeneous $(^{26}Al/^{27}Al)_o$ =5.23 x10^{-5} and homogeneous stable Mg isotopic composition in the early solar system, chondritic material with solar Al/Mg ratios must have $\mu^{26}Mg^*$ values of ~0 ppm. However, the present results for the 5 chondrules with solar-like Al/Mg show variable $\mu^{26}Mg^*$, and some of them show negative values beyond the error limit (2 σ). The results for LL chondrules tend to show $\mu^{26}Mg^*$ values even lower than those for CC chondrules. This suggests heterogeneous distribution of ^{26}Al in the early solar system.

[1] Jacobsen B. et. al. (2008) *Earth and Planet. Sci. Lett*, **272**, 353-364. [2] Larsen K. K. et al. (2011) *The Astrophysical Journal Lett*, **735**, L37. [3] Kita N. T. et al. (2013) *Meteoritics and Planet. Sci*, **48**, 1383-1400. [4] Connely J. N. et al. (2012) *Science*, **338**, 651-655. [5] Schiller M. et al. (2015) *Earth and Planet. Sci. Lett*, **420**, 45-54. [6] Luu T.-H. et al. (2015) *PNAS*, **112**, 1298-1303. [7] Olsen M. B. et al. (2016) *Geochim. Cosmochim. Acta*, **191**, 118-138. [8] Galy A. et al. (2003) *Journal of Analytical Atomic*

Spectrometry, **18**, 1352-1356. [9] Bizzarro M. et. al. (2005) *The Astrophysical Journal*, **632**, L41-L44.

Keywords: Mg isotopes, ICPMS, chondrule, CAI, early solar system

Crystal growth and disequilibrium distribution of oxygen isotopes of minerals in an igneous Ca-Al-rich inclusion from the Allende carbonaceous chondrite

*Noriyuki Kawasaki[1], Steven B Simon[2], Lawrence Grossman[2], Naoya Sakamoto[3], Hisayoshi Yurimoto[3,1]

1. ISAS/JAXA, 2. The University of Chicago, 3. Hokkaido University

Coarse-grained Ca-Al-rich inclusions (CAIs) in meteorites, the oldest objects in the Solar System (Connolly et al., 2012), exhibit unequilibrated O isotope distributions among/within minerals (e.g., Clayton et al., 1977; Clayton, 1993; Yurimoto et al., 2008 and references therein); however, the origin of the disequilibrium distribution of O isotopes remains controversial. We have observed in-situ oxygen isotope distribution and ^{26}Al–^{26}Mg systematics in a Type B1 Ca-Al-rich inclusion (CAI), TS34, from the Allende carbonaceous chondrite by using secondary ion mass spectrometry (Cameca ims-1280HR at Hokkaido University) according to crystal growth of CAI minerals and their crystal growth sequences. The heterogeneous oxygen isotope distribution among and within minerals was established by change of oxygen isotopic composition of melt during crystallization.

TS34 mainly consists of melilite, Ti-Al-rich clinopyroxene (fassaite), and spinel in addition to minor anorthite, in igneous textures, and oxygen isotopic compositions of the constituent minerals plot along the carbonaceous chondrite anhydrous mineral line. The spinel grains are uniformly ^{16}O-rich (Δ^{17}O = –22.7 ±1.7 ‰, 2SD), while the melilite grains are uniformly ^{16}O-poor (Δ^{17}O = −2.8 ±1.8 ‰) irrespective of their crystal growth. The fassaite crystals exhibit growth zoning overprinting poorly-developed sector zoning: they generally grow from Ti-rich to Ti-poor compositions. The fassaite crystals show continuous variations in Δ^{17}O along the inferred directions of crystal growth, from ^{16}O-poor (Δ^{17}O ~ −3 ‰) to ^{16}O-rich (Δ^{17}O ~ −23 ‰), which covers a full range of oxygen isotope variations of the minerals in TS34. The early-crystallized ^{16}O-poor fassaite and the melilite are in oxygen isotope equilibrium and chemical equilibrium. The oxygen isotope variations in the fassaite trace the oxygen isotope evolution of CAI melt during the fassaite crystallization, from ^{16}O-poor to ^{16}O-rich, which plausibly originated from oxygen isotope exchange with surrounding ^{16}O-rich nebular gas. The ^{16}O-poor fassaite crystalized after ^{16}O-poor melilite, while the ^{16}O-rich spinel was a relict at the melilite crystallization from ^{16}O-poor melt. These crystallization sequences are consistent with phase diagram of CAI melt crystallization. Anorthite exhibits oxygen isotope variations ranging between Δ^{17}O ~ −2 ‰and −9 ‰. The oxygen isotope variations of anorthite are essentially covered by those of fassaite, indicating co-crystallization with early to intermediate crystalized fassaite. Therefore, oxygen isotope variations of intra- and inter-minerals recorded in the CAI trace crystallization sequences of the CAI melt. The melilite and fassaite show an ^{26}Al–^{26}Mg mineral isochron proving an initial value of $(^{26}Al/^{27}Al)_0 = (5.003 \pm 0.075) \times 10^{-5}$, corresponding to a relative age of 0.05 ±0.02 Myr from the canonical. These data demonstrate that both ^{16}O-rich and ^{16}O-poor reservoirs existed in the solar nebula at least ~0.05 Myr after the birth of the Solar System.

A combined study of Be-B and Al-Mg systematics on CH and CH/CB CAIs

*Kohei Fukuda[1], Wataru Fujiya[2], Hajime Hiyagon[1], Naoji Sugiura[1], Takanori Kagoshima[3], Naoto Takahata[3], Yuji Sano[3]

1. Department of Earth and Planetary Science, Graduate School of Science, The University of Tokyo, 2. College of Science, Ibaraki University, 3. Atmosphere and Ocean Research Institute, The University of Tokyo

Beryllium-10, which decays to ^{10}B with a half-life of 1.4 Myr [1], is considered as a key indicator of irradiation processes in the Early Solar System (ESS). However, recent numerical studies [2, 3] have demonstrated that ^{10}Be can be produced by stellar processes with neutrino reactions, which rendered reconsideration of the origin of ^{10}Be in the ESS. In order to further understand the origin of ^{10}Be, it is important to determine the accurate initial abundances of ^{10}Be in several types of meteoritic components. Previous studies implied that CH and CB chondrites contain a high proportion of the outer solar system material based on their bulk Mg- and Cr-isotopic compositions and ^{15}N-rich bulk compositions [e.g., 4, 5]. If this is correct, CH and CB CAIs may have information different from CAIs in other types of chondrites. In the present study, we have conducted Be-B and Al-Mg measurements on CH and CH/CB CAIs with newly determined Be/B relative sensitivity factors using synthetic glass standards.

We studied 8 CAIs from the Sayh al Uhaymir 290 (CH) and the Isheyevo (CB/CH) chondrites. Be-B and Al-Mg measurements were conducted with a NanoSIMS 50 at Atmosphere and Ocean Research Institute (AORI), The Univ. of Tokyo. Seven out of 8 CAIs show highly variable initial ^{10}Be/^{9}Be ratios ranging from 1.1 to 33 x 10^{-4}. They cannot be explained by a molecular cloud origin [6, 7] or a stellar origin [3], suggesting that they have experienced solar cosmic ray irradiation near the proto-Sun. In contrast to Be-B systematics, all CAIs studied here do not show resolvable excesses in ^{26}Mg. This could be attributed to: (1) heterogeneous distribution of ^{26}Al in the protoplanetary disk, (2) formation prior to injection of ^{26}Al, or (3) late formation after a significant decay of ^{26}Al. (1) is unlikely because CH and CB/CH CAIs may have formed in the same region as that of CV CAIs (= near the proto-Sun) as inferred from the Be-B systematics [e.g., 8-12, this study]. (2) is possible because CH and CB/CH CAIs have highly refractory nature relative to CV canonical CAIs. (3) may be a simpler interpretation. If (3) is the case, the transportation mechanism from near the proto-Sun to the accretion region of CH and CB parent bodies must have existed at least until the timing of CH and CB/CH CAI formation.

[1] Korschinek G. et al. 2010. *Nucl. Instrum. Methods Phys. Res. B.* 268:187-191. [2] Yoshida T. et al. 2008. *ApJ.* 686: 448-466. [3] Banerjee P. et al. 2016. *Nat. Commun.* 10, 1038. [4] Van Kooten E. M. M. E. et al. 2016. *PNAS.* 113: 2011-2016. [5] Bonal L. et al. 2010. *GCA.* 74: 6590-6609. [6] Desch S. J. et al. 2004. *ApJ*: 602, 528-542. [7] Tatischeff V. et al. 2014. *ApJ.* 796,:124 (20pp). [8] McKeegan K. D. et al. 2000. *Science.* 289: 1334-1337. [9] Sugiura N. et al. 2001. *MAPS.* 36:1397-1408. [10] Chaussidon M. et al. 2006. *GCA.* 70:224-245. [11] Wielandt D. et al. 2012. *ApJ.* 748: L25 (7pp). [12] Gounelle M. et al. 2013 *ApJ.* 763: L33 (5pp).

Keywords: cosmic ray irradiation, solar protoplanetary disk, Ca, Al-rich inclusion, SIMS

Molecular and Isotope Analyses of Organic Matter in a Primitive Clast in the Zag H Chondrite

*Yoko Kebukawa[1], Motoo Ito[2], Michael E. Zolensky[3], Aiko Nakato[4], Hiroki Suga[5], Yoshio Takahashi[6], Takeichi Takeichi[7,8], Kazuhiko Mase[7,8], Queenie H. S. Chan[9], Marc Fries[3], Kensei Kobayashi[1]

1. Faculty of Engineering, Yokohama National University, 2. Kochi Institute for Core Sample Research JAMSTEC, 3. ARES, NASA Johnson Space Center, 4. Kyoto University, Division of Earth and Planetary Sciences, 5. Graduate School of Science, Hiroshima University, 6. Department of Earth and Planetary Science, Graduate School of Science, The University of Tokyo, 7. Institute of Materials Structure Science, High-Energy Accelerator Research Organization (KEK), 8. Department of Materials Structure Science, SOKENDAI (The Graduate University for Advanced Studies), 9. Planetary and Space Sciences, Department of Physical Sciences, The Open University

The Zag meteorite is a halite-bearing H3-6 chondrite [1]. The Zag contains xenolithic clast with abundant organic matter which was proposed to be originated from Ceres [2,3]. Here we report coordinated organic analyses by STXM-XANES and NanoSIMS, in order to understand the nature and origin of the organic matter. Our systematic research of the Zag clast may also provide an important linkage to the recent remote sensing observations obtained by the DAWN mission to Ceres [e.g., 4,5].
Carbon-rich areas were located in the clast grains separated from the Zag meteorite with SEM-EDS, and then lift-out sections were prepared with a FIB instrument. C, N, O-X-ray absorption near-edge structure (C,N,O-XANES) spectra of the sections (~100 nm-thick) were obtained using scanning transmission X-ray microscopes (STXM) on beamline 5.3.2.2 at Advanced Light Source, Lawrence Berkeley National Laboratory, and BL-13A at the Photon Factory, KEK. Subsequently, H, C, N, O isotopic images were collected using a CAMECA NanoSIMS 50L ion microprobe.
The STXM elemental map of C-rich region of the Zag clast shows that sub-micrometer organic grains were scattered over the FIB section, some of which have a vein-like structure. The organic matter was somewhat associated with Fe (probably Fe-sulfides). The Fe (+Ni) and C association was also observed in the clasts in Sharps (H3.4) chondrite, suggesting a potential of catalytic gas-solid reactions such as Fischer-Tropsch type (FTT) synthesis [6,7].
C-XANES spectra of the organic grains showed large peaks at 285.2 eV assigned to aromatic carbon, and at 290.3 eV assigned to carbonate (either organic or inorganic), with some features at 287.4 eV (enol C=C-OH), and 287.9 eV (aliphatic), and 288.8 eV (carboxyl). The C-XANES spectra have some similarity with organic matter from Comet Wild 2, rather than with primitive chondritic IOM [8], except for the abundant carbonate in the Zag clast.
NanoSIMS isotope imaging analyses revealed that δ^{15}N and δD have highly heterogeneous distributions within the organic matter. The average δ^{15}N value was 393 ±82 ‰with a hot spot (2639 ±722 ‰), and the average δD value was 813 ±206 ‰with a hot spot (4,150 ±1,710 ‰). The δ^{15}N was similar to the value of insoluble organic matter (IOM) from Bells (an unusual CM chondrite) and CRs, although δD was less than these IOM [9]. It may indicate that some hydrogen have been exchanged with isotopically light water in the clast parent body.
Both molecular structure and isotopic signatures indicated highly pristine (less altered) nature of organic matter in the clast, and it may be related to cometary organics and/or primitive chondritic IOM.

References: [1] Zolensky M. E. et al. (1999) *Science, 285,* 1377–1379. [2] Fries M. et al. (2013) *76th MetSoc,* Abstract #5266. [3] Zolensky M. E. et al. (2015) *78th MetSoc,* Abstract #5270. [4] Nathues A. et al. (2015) *Nature, 528,* 237–240. [5] De Sanctis M. C. et al. (2015) *Nature, 528,* 241–244. [6] Brearley A.

J. (1990) *Geochim. Cosmochim. Acta, 54,* 831–850. [7] Kebukawa Y. et al. (2017) *Geochim. Cosmochim. Acta, 196,* 74–101. [8] Cody G. D. et al. (2008) *Meteorit. & Planet. Sci., 43,* 353-365. [9] Alexander C. M. O' D. et al. (2007) *Geochim. Cosmochim. Acta, 71,* 4380–4403.

Keywords: Meteorite, Organic matter, Isotope

Oxygen isotopic ratio of the primordial water in CM chondrites

*Wataru Fujiya[1]

1. Ibaraki University, College of Science

CM chondrites are aqueously altered to various degrees in their parent body. Water ice accreted on the CM parent body reacted with primary anhydrous rock and organic matter producing secondary minerals. The O and H isotopic ratios of the primordial water are key constraints on its origin, however, they are still not well-constrained due to complex isotope exchange between water, rock, and organic matter during the aqueous alteration. Here I investigate the O isotopic ratio of the primordial water in CM chondrites based on bulk O isotopic ratios of CM chondrites and H abundances of their phyllosilicate. Most of the O and H data are from Clayton and Mayeda (1999) and Alexadner et al. (2013).
CM Falls show an apparent correlation between bulk $\delta^{18}O$ values and H abundances of their phyllosilicate. The regression line of the CM Falls passes through the representative compositions of anhydrous silicate and phyllosilicate matrix in CM chondrites, indicating a mixing line between these two components as endmembers. This well-defined mixing line strongly indicates that the O isotopic ratios of bulk CM chondrites reflect variable amounts of anhydrous silicate and phyllosilicate, i.e., degrees of alteration. A consequence from the mixing line is that phyllosilicate in CM chondrites must have a common O isotopic ratio irrespective of their alteration degrees.
Oxygen isotopic ratios of phyllosilicate are dependent not only on alteration degrees but also on water/rock ratios. Here alteration degrees (f) are evaluated as fraction of anhydrous silicate reacted, and water/rock ratios (x) are expressed as ratios of O moles in water to those in anhydrous rock. In a closed system alteration model by Clayton and Mayeda (1999), O isotopic ratios of phyllosilicate are expressed as a function of f/x based on a mass balance calculation of water, anhydrous silicate, and phyllosilicate. If there is enough water to completely alter anhydrous rock (i.e., large x), then f can range from 0 to 1. In contrast, if anhydrous rock remains after complete consumption of water (i.e., small x), f cannot reach to 1 but only take values smaller than 1 depending on x. Thus, f/x values have a maximum, when water is completely consumed by the aqueous alteration and O isotopic ratios of phyllosilicate should be the same. Given apparent occurrence of anhydrous silicate that remains unaltered, water/rock ratios are likely a limiting factor for the alteration degrees of CM chondrites. Complete water consumption is thus the most straightforward explanation for the similar O isotopic ratios inferred for CM phyllosilicate. Neither alteration temperatures nor hydration reaction considered in the calculation does this conclusion rely on. If no water remained in the system after the aqueous alteration, water/rock ratios of individual CM chondrites can be deduced from H abundances of their phyllosilicate. The deduced x values range from 0.11 to 0.29 (0.19 –0.49 by volume ratios). The variable water/rock ratios would suggest heterogeneous water ice accretion on the CM chondrite parent body.
An important implication from this scenario is the O isotopic ratio of the primordial water. In an O three-isotope plot, the O isotopic ratio of CM phyllosilicate should be on the line connecting the O isotopic ratios of the anhydrous silicate and the primordial water. Based on the mass-balance calculation by Clayton and Mayeda (1999), the inferred $\delta^{18}O$ and $\delta^{17}O$ values of the primordial water are ~65 and ~43 ‰, respectively. These estimates depend on hydration reaction considered in the calculation.

Keywords: Aqueous alteration, CM chondrite, Oxygen isotopic ratio, Primordial water

Carbonate stardust from the Murchison meteorite

*Kentaro Kudo[1]

1. TechnoPro, Inc. TechnoPro R&D Company

The formation of carbonates in meteorites is generally attributed to secondary aqueous alteration in “planetary environments” (such as Earth, Mars and asteroids), and carbonates are considered to be a good indicator of the past presence of liquid water. However, we report the first discovery of unique calcite grains embedded in the interior of a large calcium-aluminum-rich inclusion (CAI) from the Murchison CM2 carbonaceous chondrite. The individual calcite grains in the CAI are agglomerated submicron (<1 μm) crystals and coexist with high-temperature condensates such as spinel and diopside. The oxygen isotope ratios of the calcite grains have an extreme $^{17}O/^{16}O$ and $^{18}O/^{16}O$ anomaly and are clearly different from that of the secondary carbonates in the matrix. The calcite crystals have large negative anomalies with relatively heterogeneous oxygen isotope compositions ranging from −120 to +5‰ for $\delta^{17}O_{SMOW}$ and from −50 to +100‰ for $\delta^{18}O_{SMOW}$, which are extremely depleted in ^{17}O and enriched in ^{18}O relative to spinel and diopside (−45 to −40‰ for $\delta^{17}O_{SMOW}$ and −50 to −45‰ for $\delta^{18}O_{SMOW}$). Although the oxygen isotope compositions of the secondary carbonates are distributed along the TF line, those of the calcite grains in the CAI are heterogeneous and linearly distribute neither on the TF line nor near the TF line in the three oxygen isotope diagram. Therefore, our results suggest that the primitive carbonate grains may form in the proto-solar “nebular environment” without liquid water.

Keywords: Oxygen isotopes, Calcium-aluminium-rich inclusion, Molecular cloud, Proto-sun, Early solar nebula, Nano-SIMS

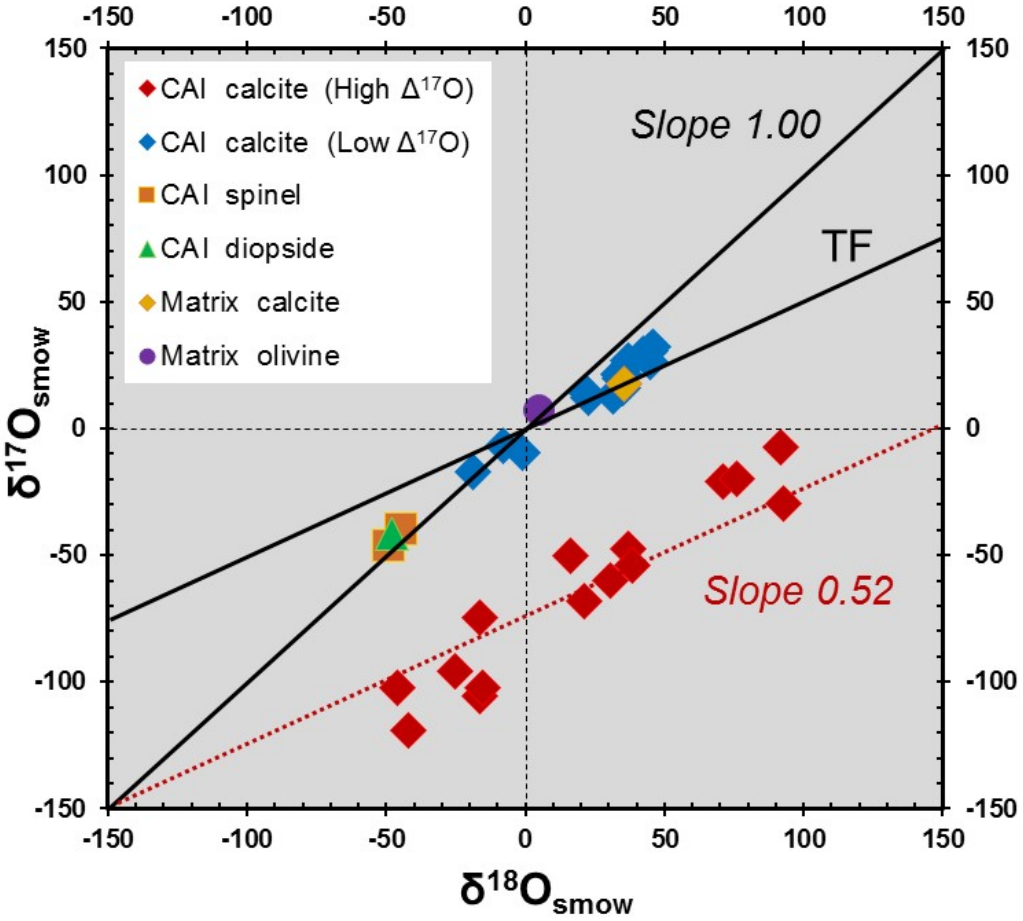

Variable shock deformation within the CV3 chondrites based on chondrule shapes determined by X-ray tomography and modes of chondrite components

*Ren Aoki[1], Timothy J. Fagan[1], Masayuki Uesugi[2], Akira Tsuchiyama[3]

1. Department of Resources and Emvironmental Engineering School of Creative Science and Engineering Waseda University, 2. Japan Synchrotron Radiation Research Institute, 3. Division of Earth and Planetary Sciences, Graduate School of Science, Kyoto University

Introduction: The high abundance of Fe,Ni-metal and high Fo-contents of olivine led to the recognition that the CV3 chondrites Efremovka, Leoville and Vigarano formed at relatively low oxygen fugacities as reduced CV3s (CV3red; [1,2]). In contrast, the CVs Allende and Axtell have little to no Fe,Ni-metal and are classified as an oxidized subgroup (CV3oxA). The CV3red subgroup is characterized by lower metamorphic grades and lower porosities than CV3oxA [3,4]. It has been proposed that the lower metamorphic grade of CV3red is due to an early impact event on the CV3 parent body that lowered porosities [5] and expelled ice [6]. In this study, we test the interpretation that the CV3red subgroup was preferentially deformed by shock by comparing (1) modes of chondrite components, (2) chondrule shapes and (3) clustering of chondrule orientations in a set of CV3red and CV3oxA chondrites.
Methods: We used elemental and BSE maps and photomicrograph mosaics of polished thin sections (pts) to determine modes of chondrite components (chondrules, CAIs, AOAs, matrix) in: one pts of Leoville; two pts of Efremovka; three pts of Vigarano; two pts of Allende and one pts of Axtell. We also determined 2-D shapes and orientations of chondrules in these pts.
Three-dimensional shapes and orientations of chondrules and chondrule-like objects were determined by X-ray computed tomography (CT) in small samples of Efremovka, Vigarano and Allende. X-ray CT data were collected using X-ray CT scanner at Kyoto University (ELESCAN, NX-NCP-C80-I; Nittetsu Elex Co.) [7]. The X-ray CT data consist of a series of 2-D images, in which pixel brightness correlates with linear attenuation coefficient (LAC) [7-8]. Elliptical shapes of low-LAC chondrules and chondrule-like objects were traced on a layer overlying each X-ray CT layer. The subsets of images of traced layers were processed using SLICE software [9] to investigate their shape using tri-axial ellipsoidal approximation and orientation of each axis of chondrules and chondrule-like objects in the samples.
Results: The ratios of matrix/inclusions ("inclusions" = chondrules + CAIs + AOAs) show a trend that correlates with the porosities of [4]. Matrix/inclusions ratios are near 0.3-0.4 for Efremovka and Leoville (porosities approx., 0.6-2%), 0.6-0.7 for Vigarano (porosity, 8%), and 0.9-1.0 for Allende (porosity, 22%). Our Axtell (porosity, 23% [4]) pts has matrix/inclusions ratio = 0.7, but a large CAI probably causes the ratio of the pts to be lower than that of Axtell as a whole. Ebel et al. [10] also found matrix/inclusions lower in Leoville and Vigarano than in Allende; however, their matrix/inclusions ratio for Allende (1.3) is higher than our results.
The 2-D pts data suggest and the 3-D X-ray CT data show that Allende chondrules tend to be spherical, and that the Efremovka and Vigarano chondrules tend to be oblate. Furthermore, the Efremovka and Vigarano chondrules have short axes with well-defined preferred orientations, consistent with flattening. The chondrite component modes, and chondrule shapes and orientations support the interpretation that the CV3red chondrites were affected by an early shock event that limited fluid-rock interaction during subsequent metamorphism [5,6]. Vigarano does not appear to be as strongly shocked as Efremovka and Leoville.
[1] McSween H.Y. (1977) GCA 41, 1777-1790. [2] Weisberg M.K. et al. (2006) *MESS 2*, Lauretta D.S. and McSween H.Y. (eds.) p. 19-52. [3] Bonal L. et al. (2006) GCA 70, 1849-1863. [4] Macke R.J. et al. (2011)

MaPS 46, 1842-1862. [5] Rubin A.E. (2012) GCA 90, 181-194. [6] MacPherson G.J. and Krot A.N. (2014) MaPS 49, 1250-1270. [7] Tsuchiyama A. et al. (2002) Geoch.J. 36, 369-390. [8] Uesugi M. et al. (2013) GCA 116, 17-32. [9] Nakano T. et al. (2006) Japan Synchrotron Radiation Research Institute. http://www-bl20.spring8.or.jp/slice/. [10] Ebel D.S. et al. (2016) GCA 172, 332-356.

Keywords: CV chondrites, shock deformation, X-ray tomography

Chondrule-cored aggregates (ChCAs): A new rock-type in CV chondrites with implications for timing of high-T crystallization events in the solar nebula

*Toshiki Yasuda[1], Timothy Fagan[1], Alexander N. Krot[2], Kazu Nagashima[2]

1. Waseda University, 2. University of Hawai'i

Introduction: Ca-Al-rich inclusions (CAIs) and amoeboid olivine aggregates (AOAs) formed by high-temperature reactions between gas and solids, and in some cases liquids, in a hot (ambient temperature > 1400K) region of the protoplanetary disk during initial stages of its evolution [1]. CAIs and AOAs in chondrites of petrologic types $\leq$3.0 tend to be ^{16}O-rich (Δ^{17}O -20‰). In contrast, chondrules formed at lower ambient temperatures (<900K) and tend to be ^{16}O-poor compared to CAIs (Δ^{17}O -10‰). Most chondrules appear to have postdated formation of CAIs and AOAs, though initial stages of chondrule formation might have overlapped with CAIs and AOAs [2,3]. Because of the later formation age of many chondrules, relict CAIs may be found included within chondrules [4], but chondrule fragments included in CAIs are very rare [5].

In this project, we describe minerals, textures and oxygen isotopes of three unusual objects from the CV3 chondrites Allende and Vigarano in which relict chondrule phenocrysts are partially enclosed by granular olivine texturally similar to AOAs. We refer to these objects as chondrule-cored aggregates (ChCAs). They are significant because their textures suggest the opposite of the conventionally accepted timing; namely, in ChCAs, an early stage of chondrule formation was apparently followed by a later stage of olivine condensation.

Methods: Two ChCAs (called NE-27 and SW-7) were identified in Allende, and one (NW-30) was found in Vigarano. Minerals and textures were characterized using petrographic microscopes, a scanning electron microscope (Hitachi S-3400N) and a JEOL JXA 8900 electron probe micro-analyzer (EPMA) at Waseda University. Oxygen isotopic compositions of olivine in the Allende ChCAs were collected using the Cameca ims-1280 SIMS at University of Hawai ‘i using conditions similar to those described in [6]. Typical uncertainty including internal and external errors is ~0.6‰ in both d^{17}O and d^{18}O.

Results: In Allende ChCA NE-27, a large (>200 μm across), low-Ca pyroxene ($En_{98}Wo_1$) similar to a chondrule phenocryst occurs in the core. The relict phenocryst is rimmed by granular olivine grains approximately < 20 μm across. The olivine grains are zoned with cores as Mg-rich as Fo_{95} and rims of approximately Fo_{60}. Olivines with compositions near Fo_{60} also occur in veins that cut across relict pyroxene. ChCA SW-7 has similar low-Ca pyroxene, granular olivine and vein olivine, but is composed of several nodules and has a more diffuse boundary with the Allende matrix. Vigarano ChCA NW-30 also has a core of low-Ca pyroxene. The granular olivine layer is not as complete as in the Allende ChCAs, but granular olivine does appear to replace low-Ca pyroxene near margins of ChCA NW-30.

SIMS oxygen isotope analyses of granular olivine from the Allende ChCAs fall near the Carbonaceous Chondrite Anhydrous Mineral and Primary Chondrule Mineral reference lines (see [7]) and form a spread of Δ^{17}O values from -8 to -3‰. All measurements are from MgO-rich cores and avoid FeO-rich olivine rims. The ^{16}O-poor isotopic composition indicates that the olivine rims of ChCAs did not form in a typical AOA-like setting. Regardless of O-isotopic setting, the ChCAs indicate (1) an early episode of chondrule formation, followed subsequently by (2) fragmentation or some process that released pyroxene phenocrysts from their host chondrules, (3) crystallization of granular olivine grains on the margins of relict phenocrysts, and (4) formation of Fe-rich olivine on rims of grains and in veins during metamorphism.

References: [1] Krot et al. (2009) GCA 73, 4963-4997. [2] Kita N.T. et al. (2005) in Krot et al. (eds) Chondrites and the Protoplanetary Disk, p. 558- 587. [3] Connelly et al. (2012) Science 338, 651-655. [4] Krot A.N. et al. (2007) MaPS 42, 1197-1219. [5] Itoh and Yurimoto. (2003) Nature 423, 728-731. [6] Nagashima K. et al. (2014) GCA 151, 49-67. [7] Ushikubo T. et al. (2012) GCA 90, 242-264.

Keywords: chondrules, solar nebula, oxygen isotopes

Development of Laser Post-Ionization SNMS for In-Situ U-Pb chronology

*Takahiro Matsuda[1], Yosuke Kawai[1], Kohei Miya[1], Jun Aoki[1], Toshinobu Hondo[1], Morio Ishihara[1], Michisato Toyoda[1], Ryosuke Nakamura[2], Kentaro Terada[1]

1. Graduate School of Science, Osaka University, 2. Office for University-Industry Collaboration, Osaka University

In space and planetary sciences, Secondary Ion Mass Spectrometer (SIMS) has been widely used for isotopic analyses at the micron scale. In the SIMS analysis, the surface of a sample is irradiated by a primary ion beam, and secondary ions of the sputtered materials are introduced into the mass spectrometer. However, the secondary ion yield of SIMS is very low (less than a few %). As a result, a large amount of material is wasted as neutral particles. In order to improve this disadvantage, we have been developing a Sputtered Neutral Mass Spectrometer (SNMS) with a femto-second laser.
The instrument consists of a focused ion beam system with a liquid metal gallium ion source (Ga-FIB) to attain an ultrahigh lateral resolution less than 1 μm. After a sputtering by Ga-FIB, the sputtered secondary particles are ionized by irradiating the femto-second laser. The post-ionized ions are introduced into the multi-turn ToF analyzer (MULTUM) which achieves ultrahigh mass resolving power of 20000. In addition, we introduced a new detection method, ion counting system, to improve the detection sensitivity. As a result of measurement of a standard sample in U-Pb chronology, 91500 zircon (concentration of uranium is about 100 ppm), the signal peaks of uranium and uranium oxides could be detected, so we have confirmed that the detection limit of the present system is 100 ppm.
In this study, we measured cyrtolite which contains a high concentration of uranium (2 wt.%) and 91500 zircon to confirm whether SNMS can be applied to in-situ U-Pb chronology. As a result of measuring two samples, uranium, uranium oxides and lead signal peaks were detected. In addition, signal peaks of interfering ions, for example, hafnium oxides and gallium clusters, were separated from the peaks of lead by increasing the number of cycles in MULTUM. After the measurement, the diameter of the sputtered area was about 1 μm. In this presentation, we will report the present performance of SNMS in in-situ U-Pb chronology.

Keywords: U-Pb chronology, SIMS, SNMS

Development of high precision Cr-Ti stable isotope measurements for extra-terrestrial materials.

*Yuki Hibiya[1], Tsuyoshi Iizuka[1], Katsuyuki Yamashita[2], Shigekazu Yoneda[3], Akane Yamakawa[4]

1. Graduate School of Science, The University of Tokyo, 2. Graduate School of Natural and Technology, Okayama University, 3. Department of Science and Engineering, National Museum of Nature and Science, 4. Center for Environmental Measurement and Analysis, National Institute for Environmental Studies

Introduction: Extra-terrestrial materials have highly variable $^{54}Cr/^{52}Cr$ and $^{50}Ti/^{47}Ti$ that do not follow mass-dependent fractionation. These variations are considered to reflect nucleosynthetic heterogeneities, possibly resulting from the incomplete and/or impermanent mixing of nuclides from different nucleosynthetic sources (e.g., 1-2). In recent years, these variations have become powerful tools for tracing astrophysical environments of early solar system (e.g., 3-4). They also provide important information about the genetic relationship between the planetary materials especially when the two isotope systems are combined (5). Here, we report the first sequential chemical separation procedure for high-precision Cr and Ti isotopic ratio measurements of extra-terrestrial rocks. We also measured Cr stable isotope compositions of the silicate samples processed through the new chemical separation scheme by thermal ionization mass spectrometry (TIMS).

Results & Discussion: Both Cr and Ti were successfully purified for standard rock samples basalt (JB-1b; 15-50 mg) and Juvinas (~20 mg) monomict non-cumulate eucrite using a new four-stage column chromatographic procedure. All the dissolved silicate samples were dried down, and re-dissolved in 2 mL of 6 M HCL for the first step of column chemistry. In the first step, Fe was separated from most elements including Cr and Ti using AG1-X8 anion exchange resin. The recovery rates in this step were 97-100% for Cr, ~100% for Ti, and 0% for Fe, respectively. In the second step, Ti-fraction was separated from Cr-fraction, and matrix elements like Ca were removed using AG50W-X8 cation exchange resin modifying the Ni separation procedure developed by (6). The recovery rates were 89-100% for Cr, 89-92% for Ti and 0% for Ca, respectively. In this step, Ti was about 43-66% left in the Cr-fraction, and Cr was about 1% left in the Ti-fraction. In the third step, Cr-fraction from the second step was further separated from Ti-fraction and purified for most matrix elements (V, Na, Mn, Mg, Na, Sr etc.) using AG50W-X8 cation exchange resin. The recovery rates in this step were 89-100% for Cr, 97% for Ti and 0% for most matrix elements. In this step, Ti and V were removed from the Cr-fraction, and about 1% of Cr and V left in the Ti-fraction. In the last step, Ti-fractions from the second step and the third step were combined, and the Ti-fraction was further purified for V and Cr. This chemical separation follows the procedure using TODGA resin described by (7). The recovery rates in this step were 97% for Ti, and 0% for Cr and V. These steps decrease the problematic isobaric interferences to be sufficiently low: $^{56}Fe/^{52}Cr$, $^{51}V/^{52}Cr$ and $^{49}Ti/^{52}Cr$ in Cr fraction were as low as 7.09×10^{-6}, 7.75×10^{-8} and 4.05×10^{-7}, respectively. The Cr stable isotope analyses yielded $\varepsilon^{54}Cr = 0.16 \pm 0.22$ (2SE) for JB-1b and $\varepsilon^{54}Cr = -0.48 \pm 0.25$ (2SE) for Juvinas. The reliability of the method was verified by the result that $\varepsilon^{54}Cr$ value for geostandard JB-1b is identical to that of Cr standard within the uncertainties. Furthermore, the $\varepsilon^{54}Cr$ value of Juvinas eucrite is identical within analytical uncertainty to the previous reported value ($\varepsilon^{54}Cr = -0.71 \pm 0.12$ (2SE); (8)). The sequential chemical separation scheme developed here allows us to extract Cr and Ti from basaltic samples with fewer steps than those in the previous study (e.g., 7,9) and with high recovery rates (>80% for all steps). We will apply the method to various extra-terrestrial materials for better understanding of the origin and evolution of the solar system.

References: (1) Trinquier et al. (2009), (2) Qin et al. (2011), (5) Warren, (2011), (6) Yamakawa et al. (2009), (7) Zhang et al. (2011), (8) Trinquier et al. (2007), (9) Schiller et al. (2014)

Keywords: Cr, Ti, nucleosynthetic anomaly, chemical separation, TIMS, eucrite

Development of integrated SR-CT method for the total analysis of meteorites

*Masayuki Uesugi[1], Akihisa Takeuchi[1], Kentaro Uesugi[1]

1. Japan synchrotron radiation research institute

Synchrotron radiation computed tomography (SR-CT) enables us to observe the internal structure of extraterrestrial materials with spatial resolution around 100nm three-dimensionally, without breaking them. In previous studies, however, we can not investigate the mineral phases and chemical composition of internal materials of the samples. In addition, considerable errors are occurred if we observed samples larger than the field of view of the CT instruments.

Recently, several methods of the combination of x-ray diffraction (XRD) and CT were developed in the material sciences of engineering fields [e.g. 1-2], and performed precise observation of polycrystalline metals or alloys. We can determine the mineral phases of the sample uniquely, orientation of the crystals inside them and analyze their chemical composition by linear attenuation coefficient [3].

In this paper, we report a new instrument for the total analysis of rocky material which includes XRD, SR-CT, and local tomography which images a region of interest of a sample by zooming up it. We also developed softwares for the integrated analysis of data obtained by the system. The software relates the images and data obtained by those different methods with simple operation. Using this system, we can search and investigate certain materials or minerals included in the sample, such as carbon phases. We also introduce future developments and application for analysis of materials obtained by future sample return missions.

References: [1] Toda et al., (2016) Acta Materialia 107 310-324. [2] West et al., (2009) Scripta Materialia 61 875–878. [3] Uesugi et al., (2013) Geochimica et Cosmochimica Acta 116, 17–32.

Keywords: synchrotron radiation tomography, XRD-CT, meteorite

3D-observation of matrix of MIL 090657 meteorite by absorption-phase tomography

*Sugimoto Miyama[1], Akira Tsuchiyama[1], Junya Matsuno[1], Akira Miyake[1], Tsukasa Nakano[2], Kentaro Uesugi[3], Akihisa Takeuchi[3], Aki Takigawa[1], Akiko Takayama[1], Keiko Nakamura-Messenger[4], Aaron S. Burton[4], Scott Messenger[4]

1. Division of Earth and Planetary Sciences, Graduate School of Science, Kyoto University, 2. AIST/GSJ, 3. JASRI/SPring-8, 4. NASA/JSC

MIL 090657 meteorite (CR2.7) is one of the least altered primitive carbonaceous chondrites [1]. This meteorite has amorphous silicates like GEMS (glass with embedded metal and sulfide), which are characteristically contained in cometary dust, in matrix [2,3] as with the Paris meteorite [4]. Three lithologies have been recognized; lithology-1 (L1) dominated by submicron anhydrous silicates, lithology-2 (L2) by GEMS-like amorphous silicates and lithology-3 (L3) by phyllosilicates [2]. Organic materials are abundant in L1 and L2 [2,3]. L1 and L2 were further divided into sub-lithology respectively based on their textures and compositions [5]. These studies were performed by 2D SEM and TEM observations of sample surfaces and thin sections that are unable to reveal what constitute each lithology and how these lithologies are distributed and related to each other. This information will provide important insights into alteration and aggregation processes on asteroids and in the early solar nebula.
In this study, MIL 090657 matrix was examined in 3D using two types of X-ray tomography; DET (dual-energy tomography) [6] and SIXM (scanning-imaging X-ray microscopy) [7]. Mineral phases can be discriminated based on absorption contrasts at two different X-ray energies in DET. In SIXM, materials composed of light elements such as water or organic materials can be identified based on phase and absorption contrasts. By combining these methods, we can discriminate not only organic materials from voids but also hydrous alteration products, such as hydrated silicates and carbonates, from anhydrous minerals [8].
In this study, we first observed cross sections of MIL 090657 matrix fragments (~100 mm) in detail using FE-SEM/EDS. Based on the results, three house-shaped samples (30~50 mm) were extracted from L1, L2 and their boundary (H1, H3 and H5, respectively) using FIB. 3D imaging of these samples were conducted at BL47XU of SPring-8, a synchrotron radiation facility, with ~30-40 nm/voxel and ~70-80 nm/voxel at 7keV and 8keV in DET and ~100 nm/voxel at 8keV in SIXM.
We found new lithologies that we named L4, L5 and L6 in H1 and H3 in addition to L1 and L2. L4. L5 and L6 are mainly composed of probably phyllosilicates with different Fe contents. Sulfide and framboidal magnetite were recognized in L4. L5 includes magnetite and carbonate and L6 includes anhydrous silicates having cracks inside. L1, L2, L4 and L5 are porous while few voids were observed in L6. L4 adjoins to L1 with boundary, which is not very distinct. L2, L5 and L6 adjoin to each other, and the boundaries of L6 with L2 and L5 are clear. In H5, coarse mineral grains (~5-10 mm) such as Fe-metal and enstatite are present in L1 and L2. L1-L2 boundary is not sharp in 3D.
In conclusion, we found a variety of lithologies by 3D observation for the first time, suggesting that the MIL 090657 meteorite experienced complex alteration and aggregation histories. As L2 is dominated by amorphous silicates, which are extremely susceptible to aqueous alteration, this is presumed to be the most primitive lithology. The contact between L2 and phyllosilicate-bearing lithologies (L5 and L6) with clear boundaries indicates that they were aggregated after aqueous alteration of L5 and L6. The indistinct boundary between L1 and L2 is suggesting that these two lithologies might originally be the same aggregate composed of amorphous silicates and coarse mineral grains. L1 might have experienced weak aqueous alteration followed by mild thermal alteration [2], while L2 did not undergo aqueous alteration.

[1] Davidson et al. 2015, 46th LPSC, 1603. [2] Cao et al. 2016, 47th LPSC, 2427. [3] Sugimoto et al. 2016, Goldschmidt Workshop on Experimental Cosmochemistry, 15. [4] Leroux et al. 2015, GCA, 170: 247-265. [5] Sugimoto et al. 2016, JAMS Ann. Congr. Abstr., 161. [6] Tsuchiyama et al. 2013, GCA, 116: 5-16. [7] Takeuchi et al. 2013, J. Synch. Rad., 20: 793-800. [8] Tsuchiyama et al. 2017, 48th LPSC, 2680.

Keywords: primitive carbonaceous chondrite, amorphous silicate, aqueous alteration

Reproduction of chondrules using ambient-controlled levitation system

*Yusuke Seto[1], Kouta Suzuki[1], Naoki Shoda[1]

1. Graduate School of Science, Kobe University

Chondrules are round (or irregular) shaped particles with sizes ranging of 0.1 −10 mm. They are mainly composed of silicates, iron metals and iron sulfides, and thought to be formed by the rapid cooling of fully or partially molten droplets before they accreted. They show unique and diverse internal micro-textures (e.g., porphyritic olivine, barred olivine, radial pyroxene, etc.) which reflect not only a composition of the stating material, but also nebular conditions, such as gas species and their partial pressures, heating and cooling rate. The conditions of chondrule formation, however, remain poorly constrained. This is mainly because the reproduction of the chondrule formation processes in a laboratory is experimentally difficult, especially in terms of a container-less arrangement and a reducing (low-fO2) ambient. In the present study, we developed gas-levitation system embedded in ambient-controlled tube furnace in order to reproduce micro-textures of chondrules, and to constrain their formation conditions.
A summary of the newly developed equipment is as follows. A vertical tube furnace with a silicon carbide heater (double coiled spiral type) and an alumina core tube (OD 50mm, ID 42 mm, referred to as “outer-tube” hereafter) was used as a heating device. An alumina inner core tube (OD 32mm, ID 26 mm, referred to as “inner-tube” hereafter) was inserted into the outer tube, and an amorphous-carbon gas-nozzle (blowout hole diameter of 1 mm) was set on at the top of the inner-tube. H_2+CO_2+Ar mixed gas were separately introduced into the both inner and outer core tubes from a gas port at the bottom of the tubes, and gas flow rates were controlled by digital mass flow controllers. The inner tube with the gas-nozzle can move up and down by a motor-controlled pantograph, and thereby the seamless switching from a sample exchange positon to maximum temperature position is possible. Levitated samples were observed by a long focal CCD camera thorough mirrors and infrared filters. To avoid lowering of the image contrast due to incandescence above 1500 K, area around the sample were irradiated by a system of high-power LED (20W) and large-aperture lens.
Using the above system, we demonstrated the containerless cooling experiments for molten silicate droplets. As stating materials, (i) natural peridotite (analogue to a Fe-poor chondrule) and (ii) oxide mixture corresponding to a type IIA (F-rich) chondrule were used. They were melted at (i) 1773 K and (ii) 1673 K for durations of ~5 min and cooled with a rate of 10^4 K/hr under a reducing condition (log fO2 = IW-1) in the above system. Surfaces and internal textures of the recovered samples were analyzed using SEM-EDX. In the recovered samples of (i), residues of original olivine (Fa~10) were surrounded by overgrown Fe-poor olivine (Fa6) with zigzag surfaces. In the molten area, both platy (10 μm thickness) and porphyritic (3-20 μm) olivines were observed. Both of them showed distinct chemical zoning and are embedded in Al_2O_3-SiO_2-rich glass. The samples of (ii) were thought to be experienced by fully molten states. They shows also both platy (100 μm thickness) and porphyritic (10-30 μm) olivine embedded in an Al_2O_3-SiO_2-rich glass. Although previous studies suggest that porphyritic chondrules were formed from partially molten states while nonporphyritic chondrules from fully molten states, the present results indicates that porphyritic texture is still possible to be formed from fully molten states. The demonstrations of the present study show that reducing-gas levitation experiments is a powerful technique to simulate the molten-quenched texture of early solar materials.

Keywords: chondrule, gas levitation , quench texture

Occurrence of Fe in sulfides, silicates and metals in enstatite and ordinary chondrites: Wide ranges in oxidation-reduction due to variations in H_2O gas?

*Yuki Tanimura[1], Timothy Fagan[1]

1. Department of Earth Sciences, School of Education, Waseda University

Introduction: Iron is one of the most abundant elements in solid materials of the solar system, and occurs in chondrites in 3 main mineral groups: silicates, metals, and sulfides [1]. Speciation of Fe between these mineral groups is an indicator of the conditions where chondrites formed in the solar nebula.
Fe-speciation of chondrites between silicates and metal indicates wide variations in oxidation state [1]. Were there similar variations in the extent of sulfidation? In this project, we use Fe speciation among silicates, metal, and sulfides in enstatite, ordinary and Rumuruti-like chondrites to address variations in oxidation, reduction and sulfidation in the part of the solar nebula where these chondrite groups formed.
Methods: We used elemental and BSE maps of polished thin sections (pts) to determine modes of minerals (enstatite, olivine, Fe,Ni-metal, troilite,…) in: Bensour (LL6), Mt. Tazerzait (L5), Tamdakht (H5), LEW 88180 (EH5), NWA 974 (E6), NWA 953 (R3). Elemental maps were collected using a JEOL JXA-8900 electron probe micro-analyzer (EPMA) at Waseda University (WU). Modes were determined manually using grids overlain on the pts maps in a graphics program. The compositions of major minerals were analyzed using the WU EPMA. We calculated moles of Fe in each mineral using the mineral compositions, published molar volumes and the modes.
We also used wet chemical analyses of chondrite whole rocks from two data sets: one collected and compiled by the Smithsonian Museum, US [2], and the other by the National Institute of Polar Research (NIPR), Japan [3]. In these analyses, FeO, Fe-metal and FeS were determined directly.
A reaction space approach [4,5] was used to identify the main reactions possible between minerals and O- and S-rich gas in E, O and R chondrites. The reacting system consists of the following phases and solid solution vectors: $NaAlSi_3O_8$, $CaMgSi_2O_6$, $MgSiO_3$, $AlAlMg_{-1}Si_{-1}$, SiO_2, O-rich gas, S-rich gas, $FeMg_{-1}$, Fe-metal, FeS, $CaAlNa_{-1}Si_{-1}$ and Mg_2SiO_4. These phases can be described by the components: Na, Ca, Mg, Al, Si, O_2, S_2 and Fe. In this system, all transfers of mass between the silicate, sulfide and metal subsystems can be described as progress along two reactions: (R_m) $Mg_2SiO_4 + 2\ FeMg_{-1} = 2\ Fe + SiO_2 + O_2$; and ($R_s$) $Mg_2SiO_4 + 2\ FeMg_{-1} + S_2 = 2\ FeS + SiO_2 + O_2$. Increasing reduction is indicated by progress on R_m, increasing sulfidation by progress on R_s, and oxidizing conditions are indicated by minor progress on both reactions. Progress on R_m is designated by X_m and ranges from 0 to 1; likewise, X_s shows progress on R_s.
Results: Fe-speciation determined from all three data sets indicate wide variations in FeO/Fe-metal (X_m from 0 to 1) and limited variations in FeO/FeS (X_s mostly from 0.1 to 0.3). The results from most oxidized to most reduced are: R-, LL-, L-, H-, E-chondrites, in agreement with [1].
Considering a model for flow of ice and other materials in the solar nebula [6], the extent of oxidation was high at an evaporation front. In this model, evaporation of H_2O-ice caused the local gas to become enriched in H_2O, increasing the oxygen fugacity of the gas. With more oxygen present in the gas, R_m could proceed to the left, transferring Fe from metal to silicates. The R chondrites could have formed just inside of the evaporation front, where the gas was enriched in H_2O-vapor. Ordinary and enstatite chondrites might have formed farther inward from the evaporation front.
References: [1] McSween H.Y. and Huss G.R. (2010) *Cosmochemistry,* Cambridge, 217-218. [2] Jarosewich E. (2006) MaPS 41:1381-1382. [3] Yanai K. and Kojima H. (1995) *Catalog of the Antarctic Meteorites*, NIPR, 230 p. [4] Thompson J.B. et al (1982) JPetrol vol. 23: 1-27. [5] Fagan T.J. and Day H.W.

(1997) Geology 25: 395-398. [6] Cuzzi J.N. and Zahnle K.J. (2004) AstrophysicalJ vol. 614: 490-496.

Keywords: chondrites, solar nebula, oxidation-reduction

Shock pressure estimation by high-pressure polymorphs and cathodoluminescence spectra of maskelynite in Yamato-790729 L6 chondrite and their significance for collisional condition

Yukako Kato[1], Toshimori Sekine[1,2], *Masahiro KAYAMA[1,3,4], Masaaki Miyahara[1,3], Akira Yamaguchi[5,6]

1. Department of Earth and Planetary Systems Science, Graduate School of Science, Hiroshima University, 2. Center for High Pressure Science and Technology Advanced Research, 3. Department of Earth and Planetary Material Sciences, Faculty of Science, Tohoku University, 4. Creative Interdisciplinary Research Division, Frontier Research Institute for Interdisciplinary Sciences, Tohoku University, 5. National Institute of Polar Research, 6. Department of Polar Science, School of Multidisciplinary Science, SOKENDAI

Most asteroidal meteorites have experienced impact events that occurred on their parent-bodies because shock-induced features (e.g., melting textures, high-pressure polymorphs and vitrification) provide clear evidences for impact events. L6 type ordinary chondrite frequently has a vein-like shock-induced melting texture (a shock-melt vein or shock vein). Furthermore, they may contain high-pressure polymorphs and shock-induced glasses (e.g., maskelynite) that were transformed from the constituent minerals (e.g., olivine, pyroxene and plagioclase) due to high-pressure and –temperature conditions induced by impact events. Such high-pressure polymorphs and shock-induced glasses provide constraints on the asteroidal impact history. In this study, Yamato (Y)-790729, which is classified as heavily shocked L6 type ordinary chondrites, was investigated to estimate the shock-pressure, temperature and size of the parent body, based on high-pressure polymorph assemblage and cathodoluminescence (CL) spectroscopy of maskelynite. The shock pressure conditions estimated by these two methods were also compared each other to evaluate the validity of the methods.

Y-790729 is a typical L6 ordinary chondrite with remnants of chondritic textures, and has a shock-melt vein. The host-rock of Y-790729 consists mainly of olivine, low-Ca pyroxene, feldspar, metallic Fe-Ni, and iron-sulfide with minor phosphate and chromite. Undulatory extinction was recognized in some plagioclase and pyroxene grains under the optical microscope. A scanning electron microscope (SEM) , laser micro-Raman spectroscopy and transmission electron microscope (TEM) equipped with an X-ray energy dispersive spectrometer (EDS) were carried out for this meteorite to determine the chemical composition, observe the petrological features and identify the high-pressure phases. Another SEM with a CL spectrometer was also conducted to characterize the shock metamorphic effects of the feldspar and maskelynite.

A shock-melt vein with a width of < ~620 μm exists in Y-790729. TEM observations and micro-Raman spectroscopy of this meteorites demonstrated that ringwoodite, majorite, akimotoite, lingunite, tuite, and xieite occurred in and around the shock-melt vein. The ringwoodite is polycrystalline assemblages under the TEM observations, where the individual grain reaches from ~0.1 to ~1.3 μm across. According to the phase equilibrium diagrams of these high-pressure polymorphs, the shock pressure in the shock-melt vein is about 14-23 GPa.

Part of plagioclase grains in the host-rock occurred as maskelynite under the optical microscope and Raman spectroscopy. Sixteen different CL spectra from maskelynite portions of Y-790729 showed characteristic emission bands at ~330 and 380 nm. The obtained CL spectral data of maskelynite portions were deconvoluted into three emission components at 2.95, 3.26, and 3.88 eV. The intensity of emission component at 2.95 eV was selected as a calibrated barometer to estimate shock pressure, and the results indicate shock pressures of about 11-19 GPa. The difference in pressure between the shock-melt vein and host-rock might suggest heterogeneous shock conditions.

Assuming an average shock pressure of 18 GPa, the impact velocity of parent-body of Y-790729 is calculated to be ~1.90 km/s. The melting temperature of the shock vein could be about 2173 K at 18 GPa, according to previous data obtained from the KLB-1 peridotite and Allende meteorite. It is likely that the duration of high-pressure and -temperature conditions recorded in the shock-melt veins of Y-790729 is several seconds, implying that the parent-body size is ~ 10 km in diameter at least, based on the incoherent formation mechanism of ringwoodite in Y-790729.

Keywords: L6 type ordinary chondrite, Yamato-790729, high-pressure polymorphs, cathodoluminescence

Discovery of heavily shocked type 3 ordinary chondrites

*Masaaki Miyahara[1], Akira Yamaguchi[2], Eiji Ohtani[3]

1. Department of Earth and Planetary Systems Science, Graduate School of Science, Hiroshima University, 2. NIPR, 3. Department of Earth Sciences, Graduate School of Science, Tohoku University

Based on the onion cell model, a parent-body of an ordinary chondrite consists of petrographic type 6, 5, 4 and 3 from inward to outward. A high-pressure polymorph occurring in a shocked ordinary chondrite gives shock pressure, temperature, impact velocity and impactor size, which become clues for understanding a destruction process of an ordinary chondrite parent-body. We have to clarify the inventories of a high-pressure polymorph included in all petrologic types to elucidate the destruction process of an ordinary chondrite parent-body. Accordingly, we will describe the petrologic and mineralogical features of the shock-induced textures and high-pressure polymorphs therein in heavily shocked type 3 ordinary chondrites.

We observed about three hundreds Antarctica type 3 ordinary chondrite (H-, L- and LL-type) petrographic thin sections stored in the NIPR under an optical microscope. We found eight type 3 ordinary chondrites with a distinct melting texture; Y-981139 (H3), A-87170 (L3), A-87220 (L3), Y-000886 (L3), Y-86706 (L3), Y-981327 (L3) A-881199 (LL3.4) and A-881981 (LL3). We also selected thirty three type 3 ordinary chondrite petrographic thin sections without a melting texture as a reference. All these samples were scanned with a field-emission scanning electron microscope (FE-SEM) to observe the fine-textures of melt-pockets and the morphologies of chondrules. Mineralogy was determined by a laser micro-Raman spectroscopy.

FE-SEM observations revealed that the melting textures (melt-pocket) in type 3 always occur around a boundary between a chondrule and matrix. Fine-grained quench silicate crystals and the spherules of metallic iron-nickel + iron sulfide with a eutectic texture filled the melt-pockets. Several interstitial glass fragments were entrained in the melt-pockets of A-881199 (LL3). Their bulk-chemical compositions are similar to that of plagioclase. Based on a Raman spectroscopy analysis, most of them are amorphous. On the other hand, back-scattered electron (BSE) image depicted that one of the interstitial glasses had a granular texture. A strong Raman shifts appeared at 372, 693 and 1032 cm-1 from the interstitial glass with a granular texture, which appear to be those of jadeite (Considering its chemical composition, probably, jadeite-diopside solid-solution) or tissintite. This is a first discovery of a high-pressure polymorph from type 3 ordinary chondrite. The ellipticity of chondrules (1 −(short axis/long axis)) in type 3 chondrites with and without a melting texture was measured. The ellipticity of chondrules in chondrites with a melting texture is ˜0.31, which appears to be a bit bigger than those of chondrules in chondrites without a melting texture. The orientation of the long axis of chondrules was also measured. The long axis of chondrules in chondrites with a melting texture appears to be oriented along a specific orientation. The ellipticity and orientation degree of chondrules besides a high-pressure polymorph would be available for estimating shock pressure condition recorded in an ordinary chondrite.

Keywords: ordinary chondrite, shock, high-pressure polymorph

Formation process of Fe-FeS globules in melt veins in shocked ordinary chondrites

*Riho Tani[1], Naotaka Tomioka[2], Kaushik Das[1]

1. Hiroshima University Department of Earth and Planetary Systems Science, 2. Kochi Institute for Core Sample Research, Japan Agency for Marine-Earth Science and Technology

Heavily shocked stony meteorites contain optically black veins called shock veins. The veins consist of micron to submicron-scale grains of silicates, oxides, Fe-Ni metals and Fe-sulfide. During shock vein formation, metal-sulfide melt is not chemically mixed with silicate melt due to their mutual immiscibility. As a result, the metal-sulfide is crystallized as tiny globules in the silicate/oxide matrix in shock veins. Such globules are an unequivocal evidence for extensive melting of silicate materials. Previously, mineralogical studies of shock vein have been mainly focused on silicate and oxide minerals, since these minerals often occur as high-pressure phases. Pressure-temperature histories in shocked chondrites have been deduced from high-pressure mineral assemblages based on experimentally determined phase equilibria [1]. However, metals and sulfides in shock veins have not been well investigated. In the present study, we have examined the Fe-FeS globules in shock veins in two ordinary chondrites (NWA4719 and Tenham), which are considered to have experienced different shock pressures, [2–3] to obtain further information of the formation process of shock veins.

The trend of the globule size in the shock vein shows that it becomes larger from the vein wall to the center (up to 25 μm) due to the difference of cooling rate and local fluid dynamics. Following the previous study [4], cooling rates of shock veins were estimated from spacing of Fe-metal dendrites in the globules by a cooling-rate meter established for Fe-dendrites in alloys [5]. The widths of Fe-dendrites in NWA4719 and Tenham are in the range of ~300–600 nm, and estimated cooling rates of the shock veins in are extremely high (10^6 deg C/sec).

To evaluate such a seemingly unrealistically high cooling rate, we examined mineral phases of the globules in Tenham by TEM/STEM. Fe-FeS globules are surrounded by high pressure silicate minerals including aluminous majorite crystallized from chondritic melt at pressures above 14 GPa. Meanwhile, X-ray elemental mapping clarified that the globules consist of grains of kamacite, taenite and troilite (<2 μm in size). But, high-pressure phases of Fe-sulfide such as Fe_3S_2 and Fe_3S, which are stable above ~14 and ~21 GPa [6,7] respectively, were not found. The results suggest that shock pressure in Tenham was significantly dropped from >14 GPa when temperature of the shock vein was in between the liquidus temperature of silicate (~2000 deg C) and eutectic temperature of Fe-FeS (~1000 deg C). Therefore, only silicate minerals could have been crystallized as high pressure phases. The absence of high-pressure phases of Fe-sulfide is rather consistent with much slower cooling rate than that estimated by Fe-dendrite spacing. The cooling-rate meter established in metallurgical studies provides overestimated values for shock veins formed in a dynamic high-pressure process.

References: [1] e.g. Agee et al. (1995) J. Geophys. Res. 100, 17725–17740. [2] Kimura et al. (2007) Meteorit. Planet. Sci. 42, 5139.pdf. [3] e.g. Tomioka and Fujino (1999) Am. Mineral. 84, 267–271. [4] Scott (1982) Geochim. Cosmochim. Acta 46, 813–823. [5] Flemings et al. (1970) J. Iron Steel Inst. 208, 371-381. [6] Fei et al. (1997) Science 275, 1621–1623 [7] Fei et al. (2000) Am. Mineral. 85, 1830–1833.

Keywords: metal-sulfide globule, shock vein, ordinary chondrite, TEM

Petrologic evidence for early impact events inferred from differentiated achondrites

*Akira Yamaguchi[1], Naoki Shirai[2]

1. National Institute of Polar Research, 2. Tokyo Metropolitan University

Eucrites, grouped in the HED meteorites are the largest group of differentiated achondrites. There are several achondrites petrologically similar to eucrites but were derived from distinct sources. Detailed petrologic and geochemical studies of such asteroidal achondrites provide better understanding of early igneous, thermal and impact histories of differentiated planetesimals. We report petrology and geochemistry of achondrites, EET 92023 and Dho 007. Oxygen isotopic compositions of these meteorites are significantly shifted away from the eucrite fractionation line. EET 92023 is an unbrecciated achondrite whereas Dho 007 is a polymict breccia mainly composed of medium to coarse-grained granular clasts. These achondrites are mainly composed of low-Ca pyroxene and plagioclase, petrologically similar to normal cumulate eucrites. However, these rocks contain significant amounts of kamacite and taenite not common in unbrecciated, crystalline eucrites. EET 92023 and Dho 007 contain significant amounts of platinum group elements (PGEs) (~10% of CI), several orders of magnitude higher than those of monomict eucrites. We suggest that the metallic phases carrying PGEs were incorporated by projectiles during or before igneous crystallization and thermal metamorphism. The projectiles were likely to be iron meteorites rather than chondritic materials, as indicated by the lack of olivine and the presence of free silica. Therefore, the oxygen isotopic signatures are indigenous, rather than due to contamination of the projectile materials with different oxygen isotopic compositions. A significant thermal event involving metamorphism after the impact event indicates that EET 92023 and Dho 007 record early impact events which took place shortly after the crust formation on a differentiated protoplanet when the crust was still hot.

Keywords: meteorites, achondrites

A petrographic study of the NWA 2924 mesosiderite

*naoji sugiura[1], makoto kimura[2], tomoko arai[1], takafumi matsui[1]

1. Chiba Institute of Technology, 2. ibaraki University

Recent chronological studies [1,2] revealed that reheating of mesosiderites occurred significantly later (~30 Ma) than the solidification of the magma ocean (~4563 Ma) on the parent body. At this age, 26-Al cannot be a significant heat source. Also, metal cannot be the heat source because even if it was derived from a core, its composition should have been fractionated by this time. (Mesosiderite metal is not fractionated in siderophile elements.) Therefore, an alternative heat source has to be looked for. Here we report petrography of a mesosiderite which was largely molten by the reheating event, based on which we discuss the heating process.

NWA 2924 has not been studied in detail. But it is noteworthy that it suffered only minor shock effects (Meteoritical Bulletin). Two polished sections (one metal nodule and one matrix) were observed with a SEM and the mineral compositions were analyzed with an EDS. The areal silicate fractions are plagioclase=0.380, pyroxene=0.534 and silica=0.086. This corresponds to the type A mesosiderite. Sub-classification of mesosiderites by degrees of reheating is rather confusing [3]. In our opinion, melt-rock mesosiderites should be classified as type 3. (Type 4 is eliminated.) They can be easily distinguished from type 2 by the absence of olivine coronas and by the presence of silica/plagioclase needles that penetrate into metal. By this definition, NWA 2924 is a type 3A mesosiderite.

Chromite in NWA 2924 shows three types of petrographic features. (1) Some chromites contain ubiquitous spherical silicate inclusions. (2) Some chromites contain similar spherical silicate inclusions which are restricted to the outer part of the chromite grains. (3) Clusters of smaller chromite grains which do not include much silicate inclusions are present. Such clusters are often observed in silicate inclusions inside metal nodules. The spherical silicate inclusions are considered to be produced as follows. Chromite and surrounding silicates were heated to above the solidus temperatures of silicates, and chromite was dissolved into the silicate melt. Shortly afterwards, it cooled rapidly and silicate melt was trapped in the growing chromite. In case (1), the heating was just enough for complete melting of chromite. In case (2), only the outer part of chromite was dissolved. In case (3), chromite was completely dissolved and the dissolved chromite component diffused away considerably, so that new chromite grains formed upon individual nucleation sites (that are located nearby), resulting in a cluster of small chromites. Such chromite features are different from those in shock-heated chondrites [4]. In shocked chondrites, chromite appears as fine (micron size) granular fragments because it is brittle.

This petrographic observation is important in 3 ways. First, it suggests that the heating was very brief. Second, it seems that chromite in metal nodules was molten more extensively, suggesting different environment such as higher temperatures and/or different melt compositions and volumes than the matrix. Third, shock heating is an unlikely mechanism for reheating mesosiderites, although it may be preferred solely based on the briefness of the heating.

Since radiogenic heat, accreting hot metal and shock heating are all ruled out as a heat source for mesosiderite reheating, we suggest that induction heating due to changing solar-wind magnetic field (joule heating by eddy current) is a plausible mechanism for mesosiderite reheating. We certainly need more observations of chromite in melt-rock mesosiderites and other shocked meteorites.

[1] M.Koike et al., G.R.L. 2017, in press. [2] M.K. Haba et al., 79th Metsoc, 2016, #6139. [3] R.Hewins, J.G.R.1984, 89, C289-C297. [4] X.Xie et al., Eur. J. Mineral. 2001, 13, 1177 - 1190.

Keywords: mesosiderite, reheating, induction

The consideration regarding formation environment of the nakhlite meteorites inferred from deformation microstructures

*Amiko Takano[1], Ikuo Katayama[1], Tomohiro Usui[2], Motoo Ito[3], Katsuyoshi Michibayashi[4]

1. Hiroshima University, 2. Earth-Life Science Institute, Tokyo Institute of Technology, 3. Kochi Institute for Core Sample Research JAMSTEC, 4. Institute of Geosciences, Shizuoka University

The nakhlite is classified as one of the Martian meteorites, and are interpreted to have originated from the Tharsis region (Treiman et al., 1987). In contrast to the Earth’ s rock, the nakhlite meteorites crystallized in thick lava flows (>125m) or in shallow intrusion (probably less than a kilometer depth), however, the details of the formation environment is still unknown (Treiman et al., 1987). Therefore, it is important to investigate the formation process and environment of the nakhlite based on comprehensive observations of crystallographic orientations in constituting minerals.
In this study, we examined a polished thin section of the Yamato 000593 nakhlite (Y000593) by mineralogical, textural and crystallographic observations using an optical microscope and electron probe micro analyzer (EPMA) at Hiroshima University and scanning microscope combined electron backscatter diffraction (SEM-EBSD) at Shizuoka University.
The Y000593 mainly composed of augite, olivine and mesostasis that is consistent with previous reports for nakhlites (e.g., Mikouchi et al., 2003). The lattice-preferred orientations for minerals in whole rock of the meteorite were determined from EBSD patterns for understanding of deformation under metamorphic conditions. We found that Y000593 has crystal preferred orientation patterns in clinopyroxenes. It is suggested that the shear stress had acted on to augites when they crystallized. Thus, we inferred the nakhlites deposited in some kind of flows such as a stream of lava that flows out of a volcano.
On the other hand, we considered the impact effect when Y000593 was ejected from Mars. In general, pyroxenes are good indicator of shock deformation, which induces mechanical twins as one of the examples of crystal defects (e.g., Mori and Takeda 1983). To estimate the effect of impact process, we measured the mechanical twin planes, which were observed in many augites in Y000593. Consequently, most of augites with mechanical twin have been formed on (100) planes. This mechanical twin is known to induce deformation in clinopyroxenes at high strain rates and moderate temperatures (Leroux et al., 2004). In comparison with the microstructural observations in experimentally shocked clinopyroxene to the results of Y000593, it is suggested that the Y000593 pyroxenes are not strongly shocked and affected by impact event. This result is consistent with a previous study that has demonstrated impact effect using degree of extinction in olivine and pyroxene in Martian meteorites (Fritz et al., 2005).

Keywords: nakhlite, crystal preferred orientation, formation environment, impact effect

Hydrogen Reservoirs in Mars as Revealed by SNC Meteorites

*Tomohiro Usui[1]

1. Earth-Life Science Institute, Tokyo Institute of Technology

The isotopic signatures of three hydrogen reservoirs are now identified based on analyses of Martian meteorites, telescopic observations, and Curiosity measurements: primordial water, surface water, and subsurface water (Usui, in press). The primordial water is retained in the mantle and has a D/H ratio similar to those seen in Martian building blocks (Usui et al. 2012). The surface water has been isotopically exchanged with the atmospheric water of which D/H ratio has increased through the planet's history to reach the present-day mean value of ~5,000‰ (Kurokawa et al. 2014). The subsurface water reservoir has intermediate δD values (~1,000-2,000‰), which are distinct from the low-δD primordial and the high-δD surface water reservoirs. We proposed that the intermediate-δD reservoir represents either hydrated crust and/or ground ice interbedded within sediments (Usui et al. 2015). The hydrated crustal materials and/or ground ice could have acquired its intermediate-δD composition from the ancient surface water reservoir (Usui et al. 2017).

References:

Kurokawa, H. et al. (2014). Evolution of water reservoirs on Mars: Constraints from hydrogen isotopes in martian meteorites. *Earth Planet. Sci. Lett.* **394**, 179-185.

Usui et al. (2012) Origin of water and mantle-crust interactions on Mars inferred from hydrogen isotopes and volatile element abundances of olivine-hosted melt inclusions of primitive shergottites. *Earth Planet. Sci. Lett.* **357-358**, 119-129.

Usui et al. (2015) Meteoritic evidence for a previously unrecognized hydrogen reservoir on Mars. *Earth Planet. Sci. Lett.* **410**, 140-151.

Usui et al. (2017) Hydrogen isotopic constraints on the evolution of surface and subsurface water on Mars. The *48th Lunar Planetary Science Conference*, Abstract #1278.

Usui et al. (in press) Hydrogen reservoirs in Mars as revealed by SNC meteorites. *Volatiles In The Martian Crust* (eds. Filiberoto J. and Schwenzer S. P.), Elsevier B.V.

Keywords: hydrogen isotope, Martian meteorites

Variations in Shock Deformation of Feldspars in Three Achondrites: NWA 2727 Lunar breccia, NWA 856 Shergottite and NWA 3117 Howardite.

*Jaeyong Lee[1], Timothy Fagan [2]

1. Department of Environmental Studies, Graduate School of Frontier Sciences, The University of Tokyo, 2. Department of Earth Sciences, School of Education, Waseda University

In this study, I investigated shock history and geochemistry of three achondrite meteorites: NWA 3117, a howardite breccia from asteroid 4 Vesta; NWA 2727, a breccia from the Moon; and NWA 856, a shergottite from Mars. Shock histories of the three meteorites were evaluated from deformation of plagioclase feldspars. Geochemical study focused on electron microprobe (EPMA) analyses of pyroxene grains and use of Mn/Fe ratios to verify classification of these samples. Feldspar grains were classified based on observations in cross-polarized light as undulatory, mosaic, mosaic-recrystallized or maskelynite. This sequence represents increasing deformation of original feldspar crystals. Undulatory crystals have wavy extinction, mosaic crystals have patchy extinction, and mosaic-recrystallized grains appear as if they were originally coarse-grained and have recrystallized to mosaics of small equant crystals. Maskelynite grains are isotropic, indicating transformation to glass. Based on feldspar deformation, the degrees of impact processing are NWA 856 > NWA 3117 > NWA 2727. All of the feldspar observed in NWA 856 is maskelynite; mosaic and mosaic-recrystallized feldspars are common in NWA 3117; and the feldspar in NWA 2727 tends to have undulatory extinction.
The high deformation of NWA 856 is expected because this sample is from Mars, which is a large parent body and requires a powerful impact to accelerate a rock to escape velocity. In contrast, the parent body of NWA 3117 (Vesta) is smaller than that of NWA 2727 (the Moon), yet NWA 3117 appears more highly deformed than NWA 2727. One possible explanation is that NWA 2727 is from a relatively young part of the Moon, which has not been exposed to impacts as long as the surface of Vesta. My EPMA analyses of pyroxenes show that Mn/Fe ratios are highest in NWA 3117, lower in NWA 856, and lowest in NWA 2727, and are consistent with classification of these meteorites as a howardite (parent body Vesta), shergottite (Mars), and lunar meteorite (Moon), respectively. The higher volatility of Mn vs. Fe suggests that the observed variations in Mn/Fe could result from parent body formation at temperatures that were highest for the Moon, lower for Mars, and lowest for Vesta. However, variations in oxygen fugacity and other parameters may also have affected Mn/Fe.

Keywords: Howardite, Shergottite, Lunar breccia, Shock deformation, Feldspar, EPMA Analysis

Validation on the scenario of the formation of asteroid belt by deuterium fusion explosion of Jupiter-like planet

*Shinji Karasawa[1]

1. Miyagi National College of Tecnology Professor emeritus

A celestial body more than 1.3% of the mass of the Sun can begin temporary fusion of deuterium [1]. Gravitational potential energy of the center of this celestial body calculated under the constant density corresponds to the temperature on deuterium is about one million degrees (10^6K). The celestial body will blast when the amount of substances emitted from the celestial body by deuterium fusion is larger than the gas being sucked by gravity.
The planet for the validation is 13 times mass of Jupiter. Orbit of the model is the same with Ceres (the center of asteroid belt:4.14x10^8 km). Distances between planets and the Sun are as follows. Neptune:45.04, Uranus:28.75, Saturn:14.29, Jupiter:7.78, planet (X):4.14, Mars:2.27, and Earth:1.50. [in 10^8 km unit]. Gravitational field of each planet was calculated at the point of the same gravity with the Sun. Values are Neptune: 0.32, Uranus: 0.19, Saturn: 0.24, Jupiter: 0.24, planet (X): 0.81, Mars: 0.013, and Earth: 0.026 [in 10^8 km unit]. Planet (X) is located at a little outside of the snow line (4.04x10^8 km [2]). Gravitational collapse is progressed in a short time due to existence of hydrogen gas about 100 times mass of dust. So, planet (X) became very large.
About 4.6 billion years ago, the Sun began the nuclear fusion. At that time, substances of solid core of the Sun were ejected into universe. Those had accelerated the growth of the planet (X). After that, the planet (X) began deuterium fusion. But, it was ended in an only blast. Most of fragments of planet (X) were emitted in the universe. Although debris that keeps the same orbital speed remains in the asteroid belt, the movement of gravitational center does not change due to elastic collision. Heavy bombardment of meteorites at 3.8 billion years before can be explained by deuterium fusion explosions of planet (X).
Further descriptions are presented at website: “https://youtu.be/QY8C7XK6k7I”, “https://youtu.be/fiMgXpUz2GQ”.

[References]

[1] Chabrier, G., Baraffe, I., Low-mass stars and substellar objects, Ann. Rev. Astron. Astrophys. 38 (2000) 337-377.
[2] Hayashi, C., Prog. Theor. Phys. Suppt., Vol. 70, pp. 35-53.

Keywords: asteroid belt, meteorite, deuterium fusion, brown dwarf, Jupiter, Ceres

Effects of protoplanetary multiplicity and migration on late-stage accretion of solids onto gas giants

*Sho Shibata[1], Masahiro Ikoma[1], Yuhiko Aoyama[1]

1. Graduate School of Science, The University of Tokyo

In recent years, many extrasolar gas giants have been discovered, and detailed observation reveals common characteristics of those gas giants. Their envelopes are thought to have come from protoplanetary disks, whose composition must be almost the same as that of central stars, namely, composed mainly of hydrogen and helium. Several studies of the bulk composition of gas giants, however, indicate that the envelopes of many gas giants, including Jupiter and Saturn, are much richer in heavy elements than the central stars. To explain the origin of the heavy elements, previous studies performed N-body simulations of planetesimals around growing gas giants and estimated the amount of heavy elements captured by gas giants. The estimated total masses are about a few Earth masses, which are too small to explain the observation. In this study, for the effects that enhance solid accretion, we take the multiplicity and migration of protoplanets into account. We demonstrate that the existence of another protoplanet can help supplying planetesimals to the protoplanet by scattering and also protoplanetary migration enhances the capture of planetesimals by sweeping. As a result, since planetesimals in broader area are captured by the planet, the envelopes end up being richer in heavy elements than previously thought.

Keywords: Heavy Elements, Planet Formation, Extrasolar Planet

Mystery of Planetary Integration Mechanism, and Origin of Moon,Asteroid Belt,Core Rich Mercury, Mystery and all Origins were unified proved by Application of Abduction at One-case Evolution with “Multi-Impact Hypothesis” to Past.

*Akira Taneko[1]

1. SEED SCIENCE Lab.

Titius Bode's law is an unenviable heuristic.However, this law has suggested the requirements of the collision coalescence of the planet each other.
When the particles of the circular orbital and the elliptical orbit are tangential collision with almost no speed difference at the far point position, they coalesce and speed decreases by thermal energy.
According to Titius Bode's law the orbital radius is expressed as Rn = Re ×(o.a + 0.4 ×2 $^{(n-1)}$). However, Re ≈149 597 870.700 km: one astronomical unit n=1 Mercury, n =2 Venus, n =3 Earth. n =4 Mars, n =5 Ceres, n =6 Jupiter, n =7 Saturn, n =8 Uranus⋯.It comes to doubt in this neighborhood
In the simulation of the giant impact hypothesis, the moon formation of only the mantle component was calculated, but the moon's orbital energy was only 1/20 of the actual one. In Abduction 's way of thinking you can explain the current situation, reliability will increase, but if you cannot explain it will increase suspicion.
In the multi impact hypothesis, since we were able to explain all of the origins of plate tectonics, the deep sea floor and the Pacific arc islands origin and the eccentricity of the Van Allen belt and the new driving force of plate tectonics in a unified way, It can be said that it could be verified by evolution and history.
In addition, ***the multi impact hypothesis*** can also explain the origins of the asteroid zone, the origin of the differentiated meteorites, the origin of Jupiter's great red spots and Pluto, the inclination of Neptune's axis, and the large origin of Mercury's core-mantle ratio. In addition to explaining the origin and evolution of the solar system in a unified way. Elucidation of the origins in the solar system physics is impossible to reproduce and it is difficult to elucidate by induction or deduction.However, if we use a physically meaningful hypothesis, the origin of the solar system also matched the initial conditions It can be said that it is closer to the truth because it can be verified by using abductions completely systematically with multiple current situations using one-time evolution.

In the simulation of hypothesis relying on no basis, there are few results and many contradictions are obtained.
In particular, in **the giant impact hypothesis**, we cannot explain the difference in density between the front and back of the moon and the origin of the meteorite heavy bombing period.
All origins can be elucidated by abduction, other proofs are difficult.
In the multi impact hypothesis, furthermore, the origin of the asteroid belt and the planetary blank of the Sera position, the core / mantle ratio of Mercury is twice that of other earth type planets, the origin of Jupiter 's large red spot, the origin of Pluto, the origin of diamond The origins of the kimber light pipe, the mysteries of the differentiated earth meteorite, the mystery of the plate movement direction sudden change, etc. can all be explained unifiedly

Keywords: Planetary accumulation mechanism, Origin of the asteroid belt, Origin of the Moon, Origin of Large Red Spot, Differentiated asteroids, core rich Mercury

チチウス･ﾎﾞｰﾃﾞの法則を再検討 (2)

8.チチウス･ボーデの法則の問題点, 8-1.本仮説での証明方法

種子彰 2016

◆水星 n＝-∞この理由が説明できない. ⇒ 禁制帯とマルチインパクト仮説.

◆小惑星帯 n＝3の欠番理由が説明できない. ⇒ CERRAの潮汐関断裂.

◆海王星 n＝7での不一致と, 冥王星の一致の理由が説明できない. ⇒CERRA断裂片のフライバイと海王星衝突

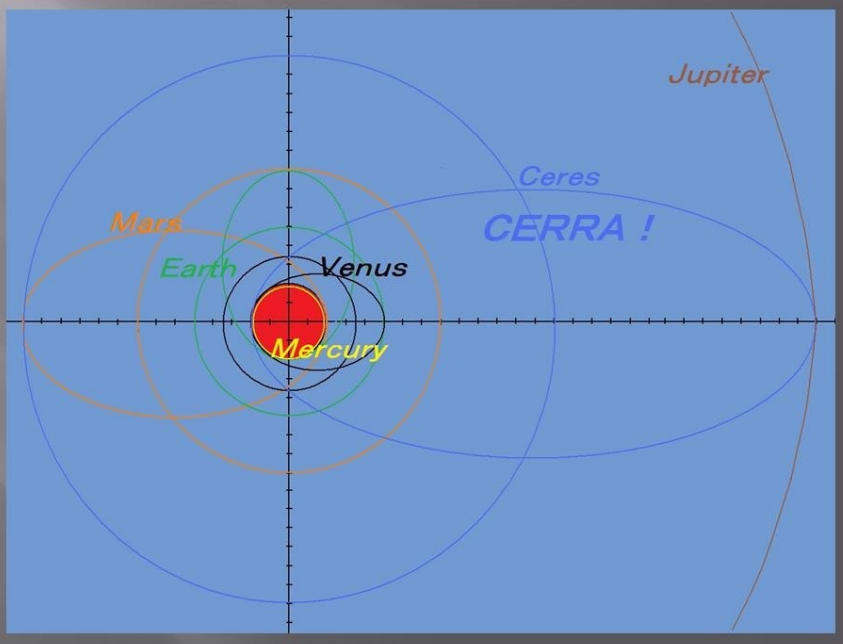

8-1.＜証明＞

●禁制帯,フィーデングゾーンでの合体

●微惑星楕円軌道道近点での衝突合体による軌道縮退

●CERRAの潮汐断裂片⇒水星に.

●断裂片木星スイングバイ⇒冥王星